

1 **The Laurentide Ice Sheet in southern New England and New York**
2 **during and at the end of the Last Glacial Maximum - A cosmogenic-**
3 **nuclide chronology**

4 Allie Balter-Kennedy^{1,2}, Joerg M. Schaefer^{1,2}, Greg Balco³, Meredith A. Kelly⁴, Michael R. Kaplan¹, Roseanne
5 Schwartz¹, Bryan Oakley⁵, Nicolás E. Young¹, Jean Hanley¹, Arianna M. Varuolo-Clarke^{1,2}

6
7 ¹Lamont–Doherty Earth Observatory, Columbia University, Palisades, NY 10964, USA

8 ²Department of Earth and Environmental Sciences, Columbia University, New York, NY 10027, USA

9 ³Berkeley Geochronology Center, Berkeley, CA 94709 USA.

10 ⁴Department of Earth Sciences, Dartmouth College, Hanover, NH 03755, USA

11 ⁵Environmental Earth Science Department, Eastern Connecticut State University, Willimantic, CT, 06226, USA

12
13 *Correspondence to:* Allie Balter-Kennedy (abalter@ldeo.columbia.edu)

14
15 **Abstract.** We present 40 new ¹⁰Be exposure ages of moraines and other glacial deposits left behind by the southeastern
16 sector of the Laurentide Ice Sheet (LIS) in southern New England and New York, summarize the regional moraine
17 record, and interpret the dataset in the context of previously published deglaciation chronologies. The regional moraine
18 record spans the Last Glacial Maximum (LGM), with the outermost ridge of the terminal complex dating to ~26–25
19 ka, the innermost ridge of the terminal complex dating to ~22 ka, and a series of smaller recessional limits within ~50
20 km of the terminal complex dating to ~21–20.5 ka. The chronology generally agrees with independent age constraints
21 from radiocarbon and glacial varves. A few inconsistencies among ages from cosmogenic-nuclide measurements and
22 those from other dating methods are explained by geologic scatter where several bedrock samples and boulders from
23 the outer terminal moraine exhibit nuclide inheritance, while *some* exposure ages on large moraines are likely affected
24 by postdepositional disturbance. The exposure-age chronology places the southeastern sector of the LIS at or near its
25 maximum extent from ~26 to 21 ka, which is broadly consistent with the LGM sea-level lowstand, local and regional
26 temperature indicators, and local summer insolation. The net change in LIS extent represented by this chronology
27 occurred more slowly (<5 to 25 m yr⁻¹) than *subsequent* retreat through the rest of New England, consistent with a
28 slow general rise in insolation and modeled summer temperature. We conclude that the major pulse of LIS deglaciation
29 and accelerated recession, recorded by dated glacial deposits north of the moraines discussed here, did not begin until
30 after atmospheric CO₂ increased at ~18 ka, marking the onset of Termination 1.

31
32 **Short Summary.** We date sedimentary deposits indicating the southeastern Laurentide Ice Sheet was at or near its
33 southernmost extent from ~26,000 to 21,000 years ago when sea-level was lowest and other climate records indicate
34 glacial conditions. Slow deglaciation began ~22,000 years ago alongside a slow but steady rise in modeled local

35 summer temperature, but significant deglaciation in the region did not begin until ~18,000 years ago when atmospheric
36 CO₂ began to rise, signaling the end of the last ice age.

37 1 Introduction

38 We describe new cosmogenic-nuclide exposure ages on moraines and other glacial-margin deposits in
39 southern New England and New York that track the timing and position of the margin of the southeastern sector of
40 the Laurentide Ice Sheet (LIS) during the Last Glacial Maximum (LGM; 26.5–19 ka) and Termination 1 (18–11 ka),
41 the most recent glacial-interglacial transition. The LIS held ~50–80 m sea-level equivalent at its greatest extent during
42 the LGM (Clark et al., 2009, 1996; Denton and Hughes, 1981; Stokes, 2017; Stokes et al., 2012), making it the largest
43 ice sheet of the last glacial period, and then deglaciated as temperature and CO₂ returned to interglacial values during
44 Termination 1 (Broecker and Donk, 1970; Cuffey et al., 2016; Dalton et al., 2020; Denton et al., 2010; Dyke, 2004;
45 Marcott et al., 2014). LIS topography, albedo, and meltwater exerted major forcing on large-scale atmospheric
46 dynamics (Löffverström et al., 2014; Ullman et al., 2014), ocean circulation (Clark et al., 2001; Denton et al., 2010;
47 McManus et al., 2004), and sea-level (Clark et al., 2009; Lambeck et al., 2014; Stokes, 2017) during the LGM and
48 subsequent deglaciation. We focus on the southeastern sector of the LIS, which is important **in part** because of its
49 proximity to the North Atlantic Ocean, meaning that meltwater from this sector had the potential to suppress the
50 Atlantic Meridional Overturning Circulation (AMOC), inducing global-scale climate feedbacks (Barker et al., 2009;
51 Barker and Knorr, 2021; Buizert et al., 2014; Denton et al., 2010; McManus et al., 2004). Improving LIS chronologies
52 **thus** bears on better understanding of regional **and hemispheric** paleoenvironmental and paleoclimatic changes.

53 Cosmogenic-nuclide and radiocarbon dating have been used to show that the LIS fluctuated at or near its full
54 LGM extent until ~22 ka, with terminal moraines dating to ~23–22 ka in the midwestern United States (Curry and
55 Petras, 2011; Glover et al., 2011; Heath et al., 2018; Ullman et al., 2015) and to ~26–24 ka in the northeastern United
56 States (Balco et al., 2002; Balco and Schaefer, 2006; Corbett et al., 2017; Stanford et al., 2021). Margin retreat
57 potentially accelerated across the LIS by ~20.5 ka (Balco and Schaefer, 2006; Ullman et al., 2015). Therefore, the
58 initial retreat of the LIS margin from its LGM limits coincided with a steady rise in boreal summer insolation that
59 began ~24 ka (Clark et al., 2009; Denton et al., 2010; Hays et al., 1976; Milankovitch, 1941; Ullman et al., 2015), and
60 began several thousand years before the deglacial rise in CO₂ observed in the Antarctic ice core record (Marcott et al.,
61 2014). The LIS might have been sensitive to this relatively weak orbital forcing in its full glacial configuration,
62 although orbital forcing alone was likely insufficient to force the return to full interglacial conditions (Barker and
63 Knorr, 2021; Denton et al., 2010; Imbrie et al., 1993; Raymo, 1997; Tzedakis et al., 2018). The increase in atmospheric
64 CO₂ beginning around 18 ka likely played a key role in the full deglaciation of the LIS (Gregoire et al., 2015; Marcott
65 et al., 2014; Shakun et al., 2015).

66 Prominent moraines in northern New Jersey, and coastal New York and New England, along with a series of
67 smaller recessional moraines, mark the LIS extent during the LGM and afford an opportunity to constrain the timing
68 of the LGM and initial deglaciation during Termination 1. These moraines are morphostratigraphically correlated across
69 the region and bracketing radiocarbon ages from a few locations have been used to estimate the ages for the entire
70 moraine sequence (Stone and Borns, 1986; Stone et al., 2005). Several of the moraine segments have now also been

Deleted: particularly

72 dated using cosmogenic nuclides (Balco et al., 2009, 2002; Balco and Schaefer, 2006; Corbett et al., 2017). Our 40
73 new ¹⁰Be ages from Rhode Island, Long Island, New York City, and the Lower Hudson Valley complement existing
74 moraine chronologies for the LIS margin and, together, these chronologies provide net changes in LIS extent as well
75 as retreat rate estimates for this climatically important sector.

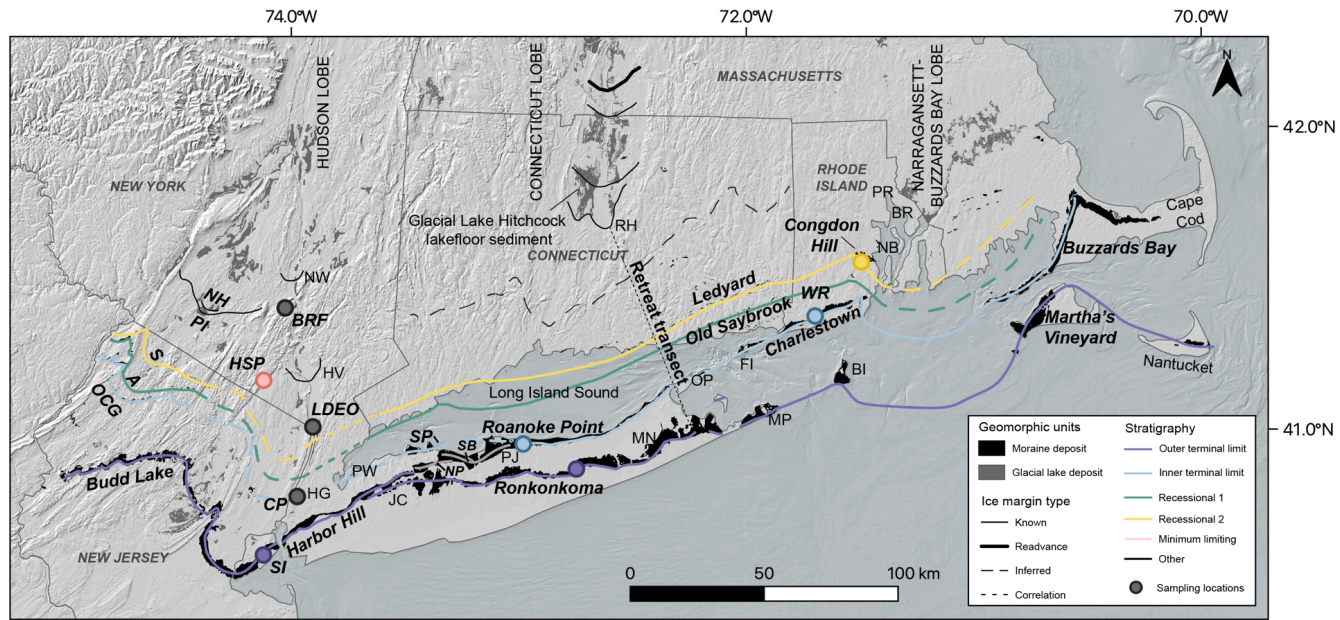
76 1.1 Existing LIS chronologies in southern New England, New York, and northern New Jersey

77 1.1.1 Regional moraine stratigraphy

78 Regional LIS margin positions have been inferred across the northeastern United States using various glacial
79 deposits, including moraines, glacial lake sediment, ice-contact deltas, and morphosequences of contemporaneous ice-
80 marginal to -distal landforms and sediment facies (e.g., Cadwell, 1989; Fuller, 1914; Koteff and Pessl, 1981;
81 McMaster, 1960; Stone and Borns, 1986; Stone et al., 2005; Woodworth and Wigglesworth, 1934). Importantly, these
82 deposits mark the most recent extension of the ice margin to a given position because each advance of the ice sheet
83 removes evidence of previous ice-margin fluctuations. The most prominent of these features is a terminal moraine
84 complex that defines the modern coastline of New England and New York, composed of two massive end moraine
85 systems that were constructed during the most extensive LGM advances of the Hudson, Connecticut, and
86 Narragansett-Buzzards Bay lobes. These large moraines (50–100 m tall, 2–10 km wide) are characterized by
87 imbricated thrust sheets of outwash deposits and dislocated preglacial sediment displaced during ice-margin advance
88 and are overlain by till in many places (Fuller, 1914; Kaye, 1972, 1964a, 1964b; Mills and Wells, 1974; Oldale and
89 O’Hara, 1984; Sirkin, 1982; Boothroyd and Sirkin, 2002). Crosscutting relationships among segments within the
90 moraine systems and, importantly, the glaciotectonic nature of the deposits combined with the presence of overlying
91 till suggest that the moraines were formed during phases of ice-margin advance as the LIS fluctuated at or near its
92 southernmost reaches during the last glaciation (Oldale and O’Hara, 1984; Sirkin, 1976; Boothroyd and Sirkin, 2002).
93 The outermost component of the terminal complex can be traced from the Budd Lake moraine in northern New Jersey,
94 to the Harbor Hill and Ronkonkoma moraines on Long Island, New York and across Block Island Sound to Martha’s
95 Vineyard and Nantucket (Figure 1; Stone and Borns, 1986). About 10–30 km north of the outer terminal limit, the
96 innermost element of the terminal moraine complex records the last major LGM ice advance in the region and is
97 correlated across Long Island’s north shore to Fisher’s Island, Connecticut, the Charlestown moraine in Rhode Island,
98 and the Buzzards Bay moraine on Cape Cod (Figure 1; Sirkin, 1976; Sirkin, 1982; Stone and Borns, 1986).

99 A series of ice-contact deltas has been used to correlate the ice-margin position along Long Island’s north
100 shore across New York City to the Ogdensburg-Culvers Gap moraine in northern New Jersey (Figure 1; Stanford,
101 1993; Stanford et al., 2021; Stone et al., 1995, 2005). The easternmost of these deltas in lower Manhattan is associated
102 with glacial Lake Bayonne, the presence of which required that the ice margin was located at or south of the Sands
103 Point moraine on Long Island to block a spillway at Hell Gate (Figure 1; Stanford et al., 2021; Stanford and Harper,
104 1991; Stone et al., 2005). The large coastal moraines dammed lakes fed by LIS meltwater as the ice-margin retreated
105 northward, and the associated lakefloor deposits are found throughout northern New Jersey (Stanford et al., 2021) and
106 underlie much of what is now Long Island Sound (Stone et al., 2005), Narragansett Bay (Oakley, 2012), Block Island
107 Sound, and Rhode Island Sound (Needell et al., 1983; Frankel and Thomas, 1966).

Deleted: .



Formatted: Indent: First line: 0"

Figure 1 - Regional map of New England and New York depicting ice marginal positions and glacial geomorphology. Hillshade topography from NASA Shuttle Radar Topography Mission (2013). Bathymetry from NOAA Office of Coast Survey BlueTopo product (tinted dark blue to indicate ocean). Glacial geology is from the surficial geologic maps of Massachusetts (Stone et al., 2018), Rhode Island (Boothroyd et al., 2003), Connecticut (Stone et al., 2005), New York (Cadwell et al., 1989), and New Jersey (Stone et al., 2002). Ice marginal positions and correlations are adapted from Sirkin (1982), Stone and Borns (1986), Boothroyd et al. (1998), Stone et al. (2005), Ridge et al. (2004), Ridge et al. (2012), and Stanford et al. (2021). Retreat rates presented in Section 5.1.3 are calculated using distance along the retreat transect. Moraine segment names discussed in the text are labeled in bold italics and other locations of relevance are labeled in regular text. Sample locations associated with a specific ice-margin position discussed in the text are colored by their stratigraphy as defined in the legend. A = Augusta moraine, BI = Block Island, BR = Barrington, RI, BRF = Black Rock Forest, CP = Central Park, FI = Fishers Island, HG = Hell Gate, HSP = Harriman State Park, HV = Haverstraw, NY, JC = Jericho, NY, LDEO = Lamont-Doherty Earth Observatory, MP = Montauk Point, MN = Manorsville, NY, NB = Narraganset Bay, NW = Newburgh, NY, NH = New Hampton moraine, NP = Northport moraine, OCG = Ogdensburg-Culvers Gap moraine, OP = Orient Point, PI = Pellets Island moraine, PJ = Port Jefferson, NY, PW = Port Washington, NY, RH = Rocky Hill, CT, S = Sussex moraine, SB = Stony Brook moraine, SI = Staten Island, SP = Sands Point moraine, WR = Wolf Rocks Moraine.

Deleted: V

Deleted: B

Ice-margin positions north of the terminal complex are marked by smaller moraines and other ice-marginal landforms that are different in character from the large coastal moraines. Several discontinuous (individual segments up to 3 km in length), boulder-rich moraines are interpreted as recording brief readvances or standstills as the Connecticut and Narragansett-Buzzards Bay Lobes retreated northward from the coastal zone (Stone et al., 2005). These include the Old Saybrook and Ledyard moraines in Connecticut, which are correlated with the Wolf Rocks and Congdon Hill moraines in Rhode Island, respectively (Figure 1; Boothroyd et al., 1998; Stone et al., 2005). The boulder-lag nature of these moraines indicates that they were affected by meltwater near the ice margin (Stone et al., 2005). Based on their morphostratigraphy, the Connecticut moraines are also tentatively correlated with the Augusta and Sussex recessional moraines in northern New Jersey (Stone and Borns, 1986; Stone et al., 2005; Figure 1). Ice-marginal positions without a moraine are marked by the collapsed ice-contact slopes of individual morphosequences deposited during deglaciation. These features mark the retreat of the ice margin in southern New England and, while they cannot be correlated across valleys for more regional ice positions, they depict systematic retreat of an active ice margin (Koteff and Pessl, 1981; Stone et al., 2005).

Deleted: ,

To summarize, two large end moraine systems comprise a terminal complex that formed during ice-margin advances as the LIS fluctuated near its maximum extent. The outermost ridges of this complex from northern New Jersey to Nantucket mark the southernmost extent of the LIS, and the innermost ridges of the terminal complex are mapped from the north shore of Long Island to Cape Cod and may be correlated with the Ogdensburg-Culvers Gap moraine in northern New Jersey. Recessional limits in Connecticut and Rhode Island are marked by smaller, discontinuous moraine segments that are starkly different in nature from the moraines of the terminal complex, and which may correlate with recessional moraines north of the Ogdensburg-Culvers Gap moraine in New Jersey.

132

133

137

138 **1.1.2 Existing chronologic constraints**

139 Numerous studies have used cosmogenic-exposure dating, radiocarbon dating, optically stimulated
140 luminescence (OSL) dating, and glacial lake sediment records to develop deglaciation histories for the LIS in southern
141 New England, New York, and New Jersey (e.g., Dalton et al., 2020; Gorokhovich et al., 2018, Halsted et al., 2022;
142 Petet et al., 2012; Ridge, 2004; Ridge et al., 2012; Stone and Borns, 1986). The timing of moraine deposition is
143 constrained by bracketing radiocarbon (^{14}C) ages in pre- and post-glacial sediment (e.g., Stanford et al., 2021; Stone
144 and Borns, 1986; Stone et al., 2005), which we have recalibrated to calendar years BP using the INTCal20 database
145 and CALIB 8.2 (Figure 2; Reimer et al., 2020). Moraines and other ice-marginal deposits dammed lakes fed by glacial
146 melt throughout the region, including Lake Albany, which occupied what is now the Hudson River Valley; glacial
147 Lake Hitchcock, in

Deleted: ion

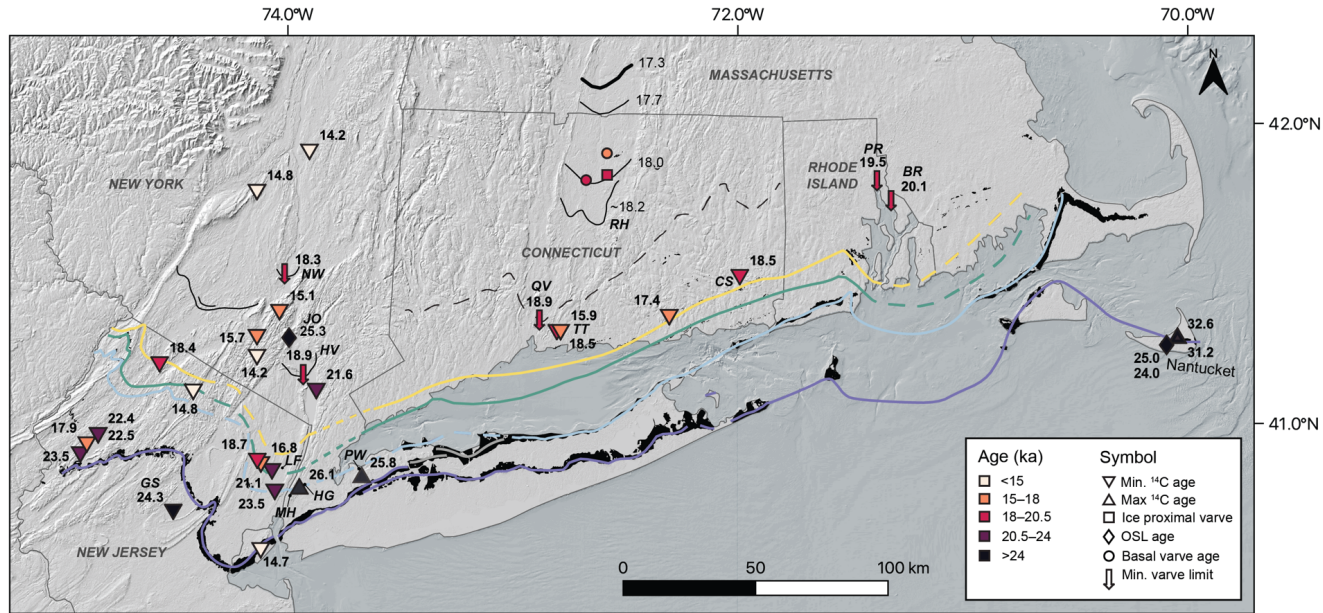


Figure 2 - Previously published chronological constraints based on radiocarbon and glacial varves. Background and ice margin limits same as Figure 1. Ages are discussed and cited in the text. Radiocarbon ages are calibrated to cal. kyr BP. BR = Barrington, RI; CS = Cedar Swamp; GS = Great Swamp; HG = Hell Gate; HV = Haverstraw, NY; JO = Pones Point; LF = Little Ferry varve sequence; MH = Manhattan, New York City; NW = Newburgh, NY; PW = Port Washington; PR = Providence River; QV = Quinnipiac Valley, CT; RH = Rocky Hill; TT = Totoket,

Deleted: same as Figure 1. Ice margin limit symbols

Deleted: , but colored in black for simplicity

Deleted: B

Deleted: PR = Providence River.

155 what is now the Connecticut River Valley; and lake Narragansett in the Narragansett Bay, Rhode Island (e.g., Antevs,
156 1928, 1922; Oakley and Boothroyd, 2013; Ridge, 2004; Ridge et al., 2012). Annually layered, or varved, sediment
157 throughout the northeast can be aligned across sites to form long varve sequences because the character and thickness
158 of varves deposited in a single year are related to climatic conditions (Antevs, 1928, 1922). These sequences yield a
159 precise chronology of ice margin retreat because (i) the presence of varves indicates ice-free conditions at a given
160 location and (ii) in some cases, a single varve can be traced across sections to its northernmost occurrence, affording
161 a maximum ice margin position for that varve year. The North American Varve Chronology (NAVC) records 5659
162 years of sediment deposition in glacial lakes in New York and New England, including Lakes Hitchcock and Albany,
163 making it the most precise and continuous terrestrial record of LIS retreat through the northeastern United States
164 (Ridge et al., 2012). Varve sequences inboard of LIS moraines also provide minimum limiting ages for those moraines.
165 The NAVC is reported in 'North American Varve Years' numbered 2701-8459, which are calibrated to calendar years
166 by radiocarbon dating of plant macrofossils and other organic material from 54 individual varves throughout the
167 chronology (Ridge et al., 2012). We report NAVC ages in years BP on the Greenland Ice Core timescale (GICC05 yr
168 BP; Andersen et al., 2006) using the offset of 20,925 years (i.e., varve year "0" equals 20,925 years BP) reported in
169 Balco et al. (2021).

170 Absolute ages have been assigned to some of the moraines using cosmogenic exposure dating (Figure 3;
171 Balco et al., 2002; Balco and Schaefer, 2006; Corbett et al., 2017). To integrate the latest developments in cosmogenic-
172 nuclide dating, and to maintain consistency with our new results in this paper, we recalculate published exposure ages
173 using v3 of the online calculator described by Balco et al. (2008), the primary production rate calibration datasets of
174 Borchers et al. (2016) and the scaling method of Lifton et al. (2014; see Methods for further discussion of production
175 rate and scaling method selection). The ages recalculated here therefore differ slightly from the originally reported
176 exposure ages from the same samples given that many of the original publications predate these updated production
177 rate calibration and scaling methods. Finally, we note that while radiocarbon ages and varve years are referenced to
178 1950 CE, the exposure ages are referenced to the time of sample collection (1995–2019 CE). This difference in
179 reference year, however, is negligible for the exposure ages discussed here, which are >18 ka.

180

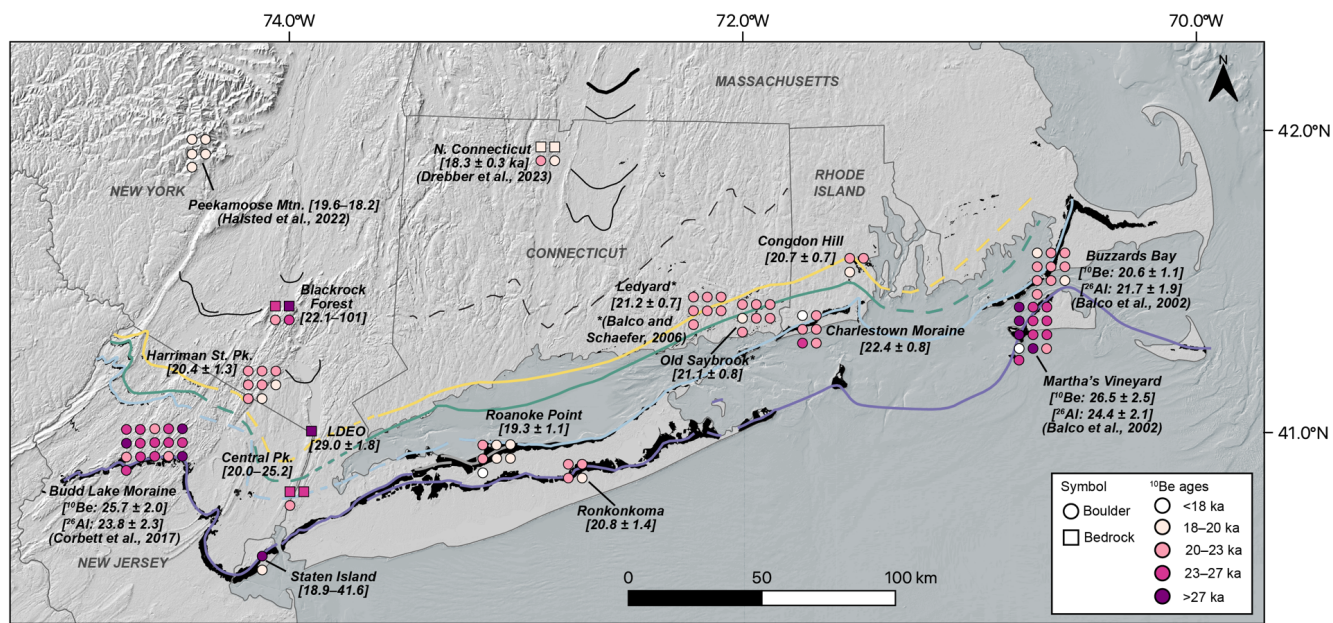


Figure 3 - New and previously published ^{10}Be exposure ages from boulder and bedrock surfaces. Background [and ice margin limits](#) same as in Figure 1. Previously published ages are listed with their reference. All are ^{10}Be ages, except where ^{10}Be and ^{26}Al ages are specified. On the Martha's Vineyard and Buzzards Bay moraines, samples with both ^{10}Be and ^{26}Al measurements are colored according to the average of the ^{10}Be and ^{26}Al ages (Balco et al., 2002). Although the Budd Lake moraine samples have both ^{10}Be and ^{26}Al measurements, the symbols are colored only by ^{10}Be age because Corbett et al. (2017) state that many of the ^{27}Al concentrations may be underestimated and therefore exclude the ^{26}Al ages from discussion. The average of the ^{26}Al ages on the Budd Lake moraine is listed for completeness. Where all samples come from the same deposit, the age is listed as mean ± standard deviation, and where samples at a site are not from the same deposit an age range is listed. A full list of sample ages is in Table 1 and moraine ages in Table 2.

183 **Connecticut and Narragansett-Buzzards Bay Lobes:** ~~Previously published~~ radiocarbon and exposure ages
184 constrain the occupation of the outer terminal limit for the Connecticut and Buzzards Bay-Narragansett Lobes to ~27–
185 25 ka. Maximum limiting radiocarbon ages in preglacial deposits near Boston and on Nantucket suggest that the LIS
186 achieved its LGM extent in the east by 32–25 ka (29–21 ¹⁴C kyr BP; n = 3; Figure 2; Oldale, 1982; Schafer and
187 Hartshorn, 1965; Tucholke and Hollister, 1973), which agrees with optically stimulated luminescence (OSL) ages
188 from Nantucket of 24.0 ± 0.9 ka on the oldest moraine and 25.0 ± 0.9 ka on the outboard outwash plain (Stone and
189 Stone, 2019; Rittenour, Stone and Mahan, 2012).

Deleted: Existing

190 ¹⁰Be and ²⁶Al ages on the Martha's Vineyard moraine range from 17.5 to 63.5 ka (n = 12) and from 17.5 to
191 60.5 ka (n = 13), respectively (Figure 3; Balco et al., 2002). Some of these exposure ages, especially those older than
192 the main age population (>30 ka), likely contain ¹⁰Be and ²⁶Al inherited from a previous exposure period (Balco et al.,
193 2002). Production of ¹⁰Be and ²⁶Al ~~attenuates~~ exponentially with depth in rock (Lal, 1991), meaning that subglacial
194 erosion of a few meters during glacial periods strips the surface of cosmogenic nuclides that accumulated during prior
195 exposure (Harbor et al., 2006). Inherited cosmogenic nuclides therefore persist in places where subglacial erosion is
196 insufficient to remove the signature of prior exposure because of minimally erosive (e.g., cold-based) ice, short ice-
197 cover durations, or both (e.g., Briner et al., 2006; Stone et al., 2003; Young et al., 2016). ~~Furthermore, the~~ LIS likely
198 remobilized boulders with significant cosmogenic-nuclide inventories at or near the terminal position as it advanced
199 towards its LGM extent, so it is not surprising that some of the exposure ages on the terminal moraine are older than
200 its true emplacement age. Large end moraines with kame and kettle topography, such as the Martha's Vineyard
201 moraine, also experience permafrost disturbance, which may expose boulders that were previously embedded in the
202 moraine and shielded from the cosmic-ray flux for some time after deposition (Applegate et al., 2010), or shift or
203 rotate boulders so original (upon deposition) top surfaces were not sampled. Exposure ages on exhumed or disturbed
204 (e.g., by agricultural practices and other human activities) boulders are therefore younger than the true emplacement
205 age of the moraine. Excluding exposure ages likely affected by nuclide inheritance or postdepositional disturbance (n
206 = 4), ¹⁰Be ages on the Martha's Vineyard moraine average 26.5 ± 2.5 ka (n = 8; mean ± standard deviation) and ²⁶Al
207 ages average 24.4 ± 2.1 ka (n = 9; Figure 3; Balco et al., 2002; Balco, 2011), and are generally consistent with the
208 maximum ~~limiting~~ radiocarbon ages in the region and the OSL ages on Nantucket.

Deleted: Al attenuates

Deleted: T

209 ¹⁰Be exposure ages on the Buzzards Bay moraine average 20.6 ± 1.1 ka (n = 10) and ²⁶Al ages average 21.7
210 ± 1.9 (n = 10; Balco et al., 2002). The Old Saybrook and Ledyard moraines in Connecticut have ¹⁰Be exposure ages
211 of 21.1 ± 0.8 (n = 7) and 21.2 ± 0.7 ka (n = 7), respectively (Figure 3; Balco and Schaefer, 2006). Thus, although the
212 moraines represent a recessional sequence and were not deposited simultaneously, their ages are indistinguishable
213 within 1σ uncertainty. Postglacial sediment containing tundra vegetation at Cedar Swamp, immediately north of the
214 Ledyard moraine, gives a minimum limiting age for the recessional moraine sequence of 18.5 ± 0.7 ka (mean age ±
215 2σ uncertainty; 15.2 ± 0.3 ¹⁴C kyr BP; McWeeney, 1995; Stone et al., 2005). A radiocarbon age of 18.5 ± 0.3 ka (15.1
216 ± 0.2 ¹⁴C kyr) at Totoket, near New Haven, Connecticut, also provides a minimum limiting age for the Ledyard
217 moraine (Figure 2; Davis et al., 1980; Deevey, 1958).

Deleted:

Deleted: c

218 Varve sequences in the region also place minimum age constraints on the recessional moraine sequence. The
219 NAVC in the Connecticut River Valley begins a few kilometers north of Rocky Hill, the spillway for glacial Lake

225 Hitchcock (Figures 1 and 2; Antevs, 1928; Ridge et al., 2012). The Rocky Hill sequence overlaps with a varve section
 226 in Newburgh, New York, which together imply that the ice margin had retreated to Newburgh and Rocky Hill by
 227 ~18.2 ka (varve year 2701; Figure 2; Antevs, 1928, 1922; Balco et al., 2021; Ridge, 2004; Ridge et al., 2012). Several
 228 varve sections south of Rocky Hill and Newburgh cannot be correlated with the NAVC and are therefore presumed
 229 older, providing minimum estimates for LIS retreat. A ~500 yr varve sequence in the Quinnipiac Valley, near New
 230 Haven, CT, is correlated with a 700-year sequence in Haverstraw, New York, placing a minimum age for ice-free
 231 conditions at Quinnipiac and Haverstraw of >18.9 ka (varve year 2000; Figure 2; Antevs, 1928; Balco and Schaefer,
 232 2006; Ridge et al., 2012). Further east, in the Providence River, Rhode Island, a 600-year varve sequence cannot be
 233 correlated with the NAVC. Summing the Providence River sequence with several varve sequences in Connecticut and
 234 southern Massachusetts between the base of the NAVC and Providence (including the Quinnipiac/Haverstraw varves),
 235 the ice margin must have retreated past Barrington, Rhode Island by ~20.1 ka and north of Providence by ~19.5 ka
 236 (Figures 1 and 2; Oakley and Boothroyd, 2013). Three cosmogenic exposure ages ~30 km north of the Rocky Hill
 237 Dam average 18.3 ± 0.3 ka, corroborating the deglaciation timing in northern Connecticut (Dreber et al., 2023).

238 The NAVC reveals [systematic net ice retreat through New England at 50–300 m yr⁻¹ \(Ridge et al., 2012\)](#),
 239 [interrupted by relatively minor advances or stillstands at least in the White Mountains and Maine, documented by](#)
 240 [comprehensive ¹⁴C-based chronologies and ¹⁰Be dating \(e.g., Borns et al., 2004; Bromley et al., 2015; Davis et al.,](#)
 241 [2015; Dorion et al., 2001, Hall et al., 2017; Kaplan, 2007; Koester et al., 2017; Thompson et al., 2017\)](#). The position
 242 of the retreating ice margin is also marked by annual DeGeer moraines spaced 100 to 300 m apart in northern New
 243 England (Sinclair, 2018; Todd, 2007; Wroblewski, 2020). [The LIS margin had retreated north of New England by 13.6](#)
 244 [ka \(Ridge et al., 2012\), with slightly later retreat or pockets of smaller residual glaciers perhaps lasting only briefly](#)
 245 [longer in areas of northern Maine \(Borns et al., 2004\)](#).

246
 247 **Hudson Lobe:** [Bulk radiocarbon ages from preglacial deposits in Port Washington, New York, and Manhattan, New](#)
 248 [York, date to \$25.8 \pm 1.6\$ ka \(\$21.8 \pm 0.8\$ ¹⁴C kyr BP\) and \$26.1 \pm 0.3\$ \(\$21.7 \pm 0.1\$ ¹⁴C kyr BP\), respectively, giving](#)
 249 [maximum limiting ages for the Hudson Lobe terminal moraine \(Figure 2; Schuldenrein and Aiuvalasit, 2011; Sirkin](#)
 250 [and Stuckenrath, 1980\). This agrees with an OSL age of \$25.3 \pm 7.4\$ ka on proglacial deposits in Jones Point, New](#)
 251 [York, associated with the advance of the Hudson Lobe \(Gorokhovich et al., 2018\). A bulk radiocarbon age of \$24.3 \pm\$](#)
 252 [1.1 ka \(\$20.2 \pm 0.5\$ ¹⁴C kyr BP\) from an LGM varve sequence at Great Swamp, New Jersey, provides a minimum](#)
 253 [limiting age for the Budd Lake moraine in New Jersey \(Figure 2; Reimer, 1984; Stanford et al., 2021\). Boulders a few](#)
 254 [km inboard of the Budd Lake moraine have ¹⁰Be ages of \$25.7 \pm 2.0\$ ka \(n = 16\) and ²⁶Al ages of \$23.8 \pm 2.3\$ ka \(n =](#)
 255 [16\), although the original publication excludes the ²⁶Al ages from discussion given evidence that the ²⁷Al](#)
 256 [concentrations were underestimated \(Figure 3; Corbett et al., 2017\). Together, the existing chronological constraints](#)
 257 [suggest that the Hudson Lobe of the LIS reached its southernmost extent by ~25–26 ka and abandoned that limit by](#)
 258 [~24 ka \(Corbett et al., 2017; Stanford et al., 2021\).](#)

259 The varves at Haverstraw, New York, place a minimum limiting age of 18.9 ka on the Ogdensburg-Culver
 260 Gap, Augusta and Sussex recessional moraines in northern New Jersey (Ridge et al., 2012). A floating varve sequence
 261 at Little Ferry in Teterboro, NJ, comprises 1100 glacial varves that must be older than the Haverstraw sequence and

Deleted: u

Deleted:

Moved (insertion) [1]

Deleted: with

Deleted: in

Moved up [1]: relatively minor advances or stillstands at least in the White Mountains and in Maine (e.g., Borns et al., 2004; Bromley et al., 2015; Davis et al., 2015; Dorion et al., 2001, Hall et al., 2017; Kaplan, 2007; Koester et al., 2017; Thompson et al., 2017)

Deleted: that the LIS margin was north of New England by 13.6 ka (Ridge et al., 2012), following relatively minor advances or stillstands at least in the White Mountains and in Maine (e.g., Borns et al., 2004; Bromley et al., 2015; Davis et al., 2015; Dorion et al., 2001, Hall et al., 2017; Kaplan, 2007; Koester et al., 2017; Thompson et al., 2017).

Deleted:

Deleted: .

Deleted: P

Deleted: is in agreement

Deleted: at Jones Point, New York

282 1430 postglacial varves that may overlap with the Haverstraw varves (Antevs, 1928, Stanford et al., 2012). The Little
283 Ferry varves therefore place a minimum limit of ~20 ka on the Augusta position (18.9 ± 1.1 kyr; Figure 2). A recent
284 compilation of chronologic constraints in northern New Jersey, places the base of the Little Ferry varve sequence at
285 ~23.5 ka based on a nearby bulk radiocarbon age (Stanford et al., 2021). Considering these varve sequences alongside
286 additional radiocarbon ages in northern New Jersey, Stanford et al. (2021) hypothesized that the Hudson Lobe
287 abandoned the terminal moraine at ~24 ka and retreated to the position of the Sussex moraine, the innermost of the
288 northern New Jersey recessional moraines, by ~23.5 ka. Based on their revised chronology, Stanford et al. (2021)
289 suggested that the Connecticut recessional moraines (Ledyard and Old Saybrook) may correlate with the New
290 Hampton and Pellets Island moraines in New York, rather than the northern New Jersey recessional sequence.

291 The earliest post-glacial radiocarbon ages on plant macrofossils in lake and bog sediment throughout the
292 region date to ~14–18.5 ka (Figure 2; Davis et al., 1980; Deevey, 1958; McWeeney, 1995; Stone et al., 2005; Peteet
293 et al., 2012). These dates provide further minimum-limiting ages for the moraine sequences discussed here. The
294 abundance of macrofossils dating to ~14–16 ka, in addition to the fact that most ages older than 16 ka come from bulk
295 sediment that are more likely to contain old carbon, has been used to argue that the LIS abandoned its LGM limit ~14–
296 16 ka (Peteet et al., 2012), and thus ~8–10 ka later than is indicated by the exposure-age and radiocarbon datasets
297 presented and compiled here.

298 **2. Geomorphology and study areas**

299 The Connecticut and Narragansett-Buzzards Bay Lobes exhibit exceptionally well preserved moraines that
300 afford an opportunity to constrain the regional timing of the LGM and its culmination. Below, we describe the
301 geomorphic settings and sample locations for 40 new exposure ages from the Connecticut and Narragansett-Buzzards
302 Bay Lobe in Long Island, New York and Rhode Island, as well as from the Hudson Lobe to the west.

303 **2.1 Connecticut and Narragansett Lobes**

304 **2.1.1 Long Island, New York**

305 Long Island is a large (~200 km long and 35 km wide), densely populated island in the New York
306 Metropolitan area that extends from Brooklyn, New York City to its eastern extents at Montauk and Orient Point
307 (Figure 1). The Island comprises tills and outwash plains associated with the southernmost extent of the LIS at the
308 LGM, and its topography is defined by several prominent moraine ridges (>60 m relief, at points), including the
309 Ronkonkoma, Harbor Hill and Roanoke Point moraines (Figure 1; Fuller, 1914; Sirkin, 1982; Sirkin and Stuckenrath,
310 1980). The Ronkonkoma moraine is the stratigraphically oldest (southernmost) associated with the Connecticut Lobe
311 of the LIS and extends E-W from the hamlet of Jericho in west-central Long Island to Montauk, forming the South
312 Fork of Long Island. The moraine ridge comprises discontinuous kame deposits and thrust sheets overlain by thin,
313 sandy till and bisected by outwash-filled valleys (Cadwell, 1989; Sirkin 1982). The easternmost point of the
314 Ronkonkoma moraine at Montauk Point is correlated with the outer terminal moraine positions on Block Island,
315 Martha's Vineyard, and Nantucket (Stone and Borns, 1986; Sirkin, 1976). Although boulders ideal for surface

Deleted:

317 exposure dating were difficult to locate on the Ronkonkoma moraine, we sampled four medium-sized (~1 m height)
318 ~~granio~~d boulders near Manorville, NY (Figure S1).

319 The Harbor Hill moraine was originally ~~correlated with the~~ New Jersey ~~terminal position, mapped as~~
320 ~~extending from~~ Staten Island and across the north shore of Long Island, crosscutting the Ronkonkoma moraine near
321 Jericho, New York (Fuller, 1914; Figure 1). Yet, updated models of Long Island glaciation demonstrate that the
322 classical Harbor Hill moraine comprises several segments ~~that may have been~~ deposited asynchronously (Sirkin, 1982;
323 Stone and Borns, 1986). Here, the term Harbor Hill moraine refers to the segment extending from the confluence with
324 the Ronkonkoma moraine through Staten Island, which represents the terminal limit of the Hudson Lobe in western
325 Long Island (Figure 1), while the Northport ~~Stony Brook~~ moraine segments northeast of the confluence with the
326 Ronkonkoma moraine are considered younger positions (Sirkin, 1982; Stone and Borns 1986). A stratigraphic section
327 in Port Washington, New York, reveals that the Harbor Hill moraine is characterized by ablation till up to 10 m thick
328 overlying thrust sheets of stratified drift containing dislocated preglacial deposits, suggesting it formed during a
329 readvance (Mills and Wells, 1974; Oldale and O'Hara, 1984). Several additional moraine segments are mapped north
330 of the Ronkonkoma ice-margin position in eastern Long Island (Sirkin 1982; Sirkin, 1998), which are not discussed
331 further here.

332 The Roanoke Point landform is the innermost Connecticut Lobe moraine on Long Island. It appears to
333 crosscut the Stony Brook moraine segment near Port Jefferson, New York, extending east to Orient Point, forming
334 the North Fork of Long Island (Figure 1; Cadwell, 1989; Sirkin, 1982). The moraine consists of till over deformed
335 outwash (Sirkin, 1982). Glaciotectonic structures, ~~such as imbricated thrust sheets and dislocated strata~~, within the
336 moraine stratigraphy indicate that the moraine was likely deposited during a readvance of the ice margin, rather than
337 a representing a standstill (Oldale and O'Hara, 1984; Boothroyd and Sirkin, 2002). The Roanoke Point moraine is
338 correlated with the Sands Point moraine to the west, deposited by the Hudson Lobe, and tentatively correlated with
339 the Odgensburg-Culvers Gap moraine in northwest New Jersey (Figure 1; Section 1.1.1; Stanford, 2010, 1993;
340 Stanford et al., 2021; Stanford and Harper, 1991; Stone et al., 2002, 1995). We sampled seven large (>1 m tall, with
341 some as tall as 4 m) erratic boulders ~~on or near~~ the Roanoke Point moraine in the vicinity of Port Jefferson, New York,
342 ~~and~~ Stony Brook University (Figure 4; Figure S1).

343 Mapping and sampling of the Long Island moraines was undertaken through the Lamont-Doherty Earth
344 Observatory Undergraduate Student Summer Intern Program between 2002-2006. Original field observations from
345 2006 note that one sample, LI-9, is located in a topographic depression, and may have been exhumed or toppled after
346 deposition. Upon further inspection in 2023, many of the samples collected from the Roanoke Point moraine are
347 located in topographic low points, and only LI-1 and LI-8 were taken from local high points where boulders were less
348 likely to have been affected by postdepositional processes (Figure S1).

349

Deleted: te

Deleted: mapped as extending from

Deleted: to

Deleted: and

Deleted: on

Deleted: near



Figure 4 - Representative sampling locations for surface exposure dating. LI-3: Large boulder sampled in an urban setting of the Roanoke Point moraine on Long Island. The sizable boulder is slightly off the moraine crest (in the background), not located on a local high point and may have experienced postdepositional disturbance. GB2002-CH-4: stable boulder on the Charlestown moraine. Ledyard Moraine: interlocked boulders of the Ledyard moraine in Connecticut. Harriman State Park: Interlocked boulders forming an ice-marginal boulder deposit.

Deleted: 6

356

357 2.1.2 Rhode Island

358 Three ice marginal positions in southern Rhode Island are marked by the Charlestown, Wolf Rocks and
 359 Congdon Hill moraines. The stratigraphically oldest is the Charlestown moraine, which is part of the Roanoke Point
 360 - Fishers Island - Charlestown - Buzzards Bay limit (Figure 1; Kaye, 1960; Upham, 1879). The moraine is ~30 km by
 361 0.5–3 km wide, rising as much as 30 m above the surrounding topography (Kaye, 1960). It is composed of a mixture
 362 of diamict and glaciotectonically displaced stratified deposits (sand and gravel), suggesting it formed during a
 363 readvance, with numerous large boulders at the surface (Boothroyd et al., 1998; Boothroyd et al., 2002; Oldale and
 364 O’Hara, 1984; Schafer, 1965). The Wolf Rocks boulder moraine, which we did not sample, is inboard of the
 365 Charlestown moraine and is correlated with the Old Saybrook recessional moraine in Connecticut (Stone et al., 2005).
 366 The Congdon Hill moraine is the innermost recessional moraine in Rhode Island and is correlated with the Ledyard
 367 recessional moraine in Connecticut to the west (Boothroyd and Sirkin, 2002; Stone et al., 2005). This hummocky

369 moraine ridge is 6 km long and 3–20 m in height and comprises boulders and sandy till, with numerous large boulders
370 near the moraine crest (Stone, 2014).

371 We collected six samples on the Charlestown moraine, and three samples on the Congdon Hill moraine, all
372 of which were from large (>1 m) boulders (Figure 4; Figure S2). Field observations note that sample GB2002-CH-1
373 on the Charlestown moraine was collected from a boulder that had collapsed into a gravel pit. Although it appeared
374 that its original position could be reconstructed from weathering characteristics and other evidence, this could not be
375 verified.

376

377 2.2 Hudson Lobe

378 The Hudson Lobe of the LIS deposited a NE-SW trending moraine on Staten Island that correlates with the
379 terminal moraines on Long Island to the east (Figure 1; Cadwell, 1989) and in northern New Jersey to the west (Stone,
380 2002). The hummocky moraine is 0.5–4 km wide by 20 km long, comprising primarily reddish-brown, clayey tills
381 that are up to ~45 m thick (Soren, 1988). Boulders are rare on the moraine crest (Soren, 1988), but we found two
382 granite boulders suitable to sample (Figure S3).

383 We also present new exposure ages from several locations in the Lower Hudson Valley at Central Park in
384 New York City, Lamont-Doherty Earth Observatory (LDEO), Harriman State Park, and Black Rock Forest (Figure
385 1). Glacially molded outcrops of Manhattan Schist in Central Park, New York City, 25 km north of the terminal
386 moraine, are sparsely overlain by erratic boulders sourced from pegmatitic granites that outcrop ~15 km north of
387 Central Park near the Bronx Zoo (Brock and Brock, 2001; Jaret et al., 2021; Taterka, 1987). We sampled two quartz
388 veins within Manhattan Schist, one from Umpire Rock at the southwest corner of Central Park, and one in the
389 northwest corner of the park, as well as a boulder from the southeast corner of the Sheep Meadow (Collins, 2005). At
390 LDEO, ~50 km north of the terminal limit, we collected a single sample for surface exposure dating from the Palisades
391 diabase. At Harriman State Park, ~70 km north of the terminal moraine, we sampled eight large (generally >2 m tall)
392 gneiss or granitoid boulders from an area with a large concentration of erratics, representing a local ice-marginal
393 deposit, in an area near two large boulders called the Grandma and Grandpa Rocks (Figure 4). The erratics are perched
394 on bedrock, or on top of thin till veneer. Finally, at Black Rock Forest, ~90 km north of the outer terminal limit, we
395 collected three samples of glacially eroded gneissic bedrock and two samples from large (>2 m tall) granite boulders.

396 3 Methods

397 Samples for surface exposure dating from the upper surfaces of bedrock and erratic boulders were collected
398 between 2002 and 2006 using the drill-and-blast method of (Kelly, 2003) and/or hammer and chisel. We collected one
399 replicate sample at Black Rock Forest (BRF-19-01) in 2019. At each site, we measured topographic shielding using a
400 clinometer and recorded the sample location and elevation using handheld GPS, except for the samples from Rhode
401 Island for which elevations were measured by barometer traverse from the nearest USGS benchmark. Samples were
402 processed at the Lamont-Doherty Earth Observatory cosmogenic dating laboratory following established procedures
403 for isolating quartz and extracting beryllium (e.g., Schaefer et al., 2009). $^{10}\text{Be}/^9\text{Be}$ ratios were measured at the Center

Deleted: at

405 for Mass Spectrometry at Lawrence Livermore National Laboratory (LLNL-CAMS) between August 2005 and July
406 2007, with one additional measurement in July 2019. Prior to 2007, samples were measured relative to the KNSTD
407 standard with a $^{10}\text{Be}/^9\text{Be}$ ratio of 3.11×10^{-12} (Nishiizumi, 2002). Measurements in 2007 or later were made relative
408 to the 07KNSTD standard with a $^{10}\text{Be}/^9\text{Be}$ ratio of 2.85×10^{-12} (Nishiizumi et al., 2007), which is taken into account
409 for our ^{10}Be age calculations (Balco et al., 2008). ^{10}Be concentrations ranged from 5.61×10^4 to 6.17×10^5 with
410 analytical uncertainty of 2–9%. Blank corrections, calculated by subtracting the average number of ^{10}Be atoms from
411 blanks processed in each sample batch, ranged from <0.5–12%, with the majority of blank corrections being <2%
412 (Table S1). Reported uncertainties in ^{10}Be concentrations include analytical errors, blank errors, and uncertainties
413 related to the ^9Be concentration (1.5%) propagated in quadrature.

414 Apparent ^{10}Be exposure ages are calculated using Version 3 of the online exposure calculator described by
415 Balco et al. (2008) and subsequently updated, with all information needed to calculate exposure ages available at
416 <https://version2.ice-d.org/laurentide/publication/1187/>. Here, “apparent” exposure ages refer to the calculated surface
417 age assuming a single period of exposure with no erosion or burial. We note that including the effects of subaerial
418 rock erosion or snow cover would make the ages presented here slightly older. Since the publication of the first
419 exposure age chronologies in southern New England, efforts have been made to better estimate cosmogenic-nuclide
420 production rates at sites with independent age control (e.g., Balco et al., 2009; Kaplan et al., 2011; Putnam et al., 2019;
421 Young et al., 2013). Of particular relevance here, Balco et al. (2009) established a regional ^{10}Be production rate
422 calibration dataset for northeastern North America (NENA) using ^{10}Be measurements at independently dated sites in
423 New England, most of which are part of the NAVC, and on Baffin Island, Canada. In an effort to synthesize several
424 new and existing production rate datasets, Borchers et al. (2016) describe “primary” production rate datasets for ^{10}Be
425 and ^{26}Al (among other nuclides), which includes sites that range in latitude and elevation, but does not include
426 calibration sites from NENA. As of this writing, the ^{10}Be reference production rates calculated using the NENA and
427 Borchers et al. (2016) datasets differ by only ~1.5% (reference production rates calculated in the online production
428 rate calculator described by Balco et al. (2008) and subsequently updated
429 (http://hess.ess.washington.edu/math/v3/v3_cal_in.html; last access January 26, 2023). Given the similarity of these
430 two production-rate datasets, we here employ the ^{10}Be and ^{26}Al production rates of Borchers et al. (2016) to avoid
431 circularity when discussing the agreement of the exposure age chronology with the NAVC. In addition, time-
432 dependent production rate scaling frameworks, which account for changes in the geomagnetic field (and therefore
433 cosmic ray flux to the Earth’s surface), have been more widely adopted. The LGM moraines discussed here have
434 exposure ages older than those at the production rate calibration sites (Balco et al., 2009; Borchers et al., 2016), so
435 employing time dependent scaling methods may produce more accurate exposure ages. Therefore, we discuss
436 exposure ages calculated using the primary production rate calibration dataset of Borchers et al. (2016) and time-
437 dependent “LSDn” production rate scaling method of Lifton et al. (2014), although also provide ages calculated using
438 the NENA production rate calibration dataset of Balco et al. (2009; NENA) and non-time-dependant “St” scaling (Lal,
439 1991; Stone, 2000) in Tables S2 and S3. We recognize that the choice of scaling method affects moraine absolute
440 exposure ages by up to ~5% (Table 2), but emphasize this is within the uncertainty of many moraine ages, and does
441 not affect the calculated rates of net retreat between moraines nor our conclusions.

Deleted: <https://version2.ice-d.org/laurentide/>

Deleted: w

Deleted: a few percent

Deleted: which

Deleted: but

447 **4 Results**

448 Exposure ages from Long Island, New York, and Rhode Island, which are presented in Table 1 and Figure 3,
449 are relevant to the glacial history of the Connecticut and Narragansett-Buzzards Bay Lobes of the LIS. Ages on the
450 Ronkonkoma moraine range from 19.1 to 22.4 ka, with an average of 20.8 ± 1.4 ka (average \pm SD; $n = 4$). Boulders
451 on the Roanoke Point moraine range in age from 18.2 to 20.9 ka, averaging 19.3 ± 1.1 ka ($n = 6$), with one outlier
452 that is 14.2 ± 0.6 ka. In Rhode Island, six boulders on the Charlestown moraine have exposure ages that range from
453 21.8 to 23.7 ka, with one outlier (GB2002-CH-1) excluded because field observations indicated the boulder may not
454 have been in its original position (Section 2.1.2), as confirmed by an exposure age (17.4 ± 1.6 ka) younger than the
455 main population of ages on this moraine. The average age of the Charlestown moraine is 22.4 ± 0.8 ka ($n = 5$).
456 Boulders on the Congdon Hill moraine range in age from 20.0 to 21.3 ka, and average 20.7 ± 0.7 ka ($n = 3$).

457 Additional exposure ages west of Long Island in southern New York, pertain to the Hudson Lobe of the LIS
458 (Figure 3). On Staten Island, two boulders yield ^{10}Be ages of 41.6 ± 2.4 and 18.9 ± 2.1 ka. In Central Park, Manhattan,
459 two ^{10}Be ages from bedrock samples are ~~25.0 ± 0.7~~ and 23.2 ± 0.8 and an erratic boulder from Sheep Meadow yields
460 an age of 20.0 ± 0.7 ka. A single ^{10}Be age on bedrock at the Lamont-Doherty Earth Observatory is 29.0 ± 1.8 ka.
461 Samples from the ice-marginal deposit in Harriman State Park range in age from 18.7 to 22.8 ka, averaging 20.4 ± 1.3
462 ka ($n = 8$). Finally, three bedrock samples at Black Rock Forest date to 25.0 ± 0.7 , 102 ± 3 , and 101 ± 3 ka (the latter
463 two bedrock samples are from the same outcrop), and two boulder samples date to 23.7 ± 0.8 and 22.1 ± 0.8 ka.

464
465
466
467
468
469
470
471
472
473
474
475
476
477
478
479
480
481

Deleted: on Umpire Rock
Deleted: 2
Deleted: 8

Table 1 - New ^{10}Be exposure ages in southern New England and New York. All ages calculated using the primary production rate dataset of Borchers et al. (2016)

| Sample ID | Sample type | ^{10}Be Age LSDn scaling (yrs) | ^{10}Be age internal error LSDn Scaling (yrs) | ^{10}Be Age St scaling (yrs) | ^{10}Be age internal error St Scaling (yrs) | Included in landform age reported in Table 2? |
|---|-------------|---|--|---------------------------------------|--|---|
| Connecticut Lobe | | | | | | |
| <i>Ronkonkoma Moraine, Long Island, NY</i> | | | | | | |
| LI-10 | boulder | 22400 | 800 | 21600 | 700 | yes |
| LI-11 | boulder | 20700 | 700 | 19700 | 600 | yes |
| LI-13 | boulder | 21100 | 700 | 20100 | 700 | yes |
| LI-14 | boulder | 19100 | 800 | 18000 | 700 | yes |
| <i>Roanoke Point Moraine, Long Island, NY</i> | | | | | | |
| LI-1 | boulder | 20100 | 1000 | 19100 | 900 | yes |
| LI-3 | boulder | 19800 | 600 | 18800 | 600 | yes |
| LI-4 | boulder | 18300 | 600 | 17300 | 500 | yes |
| LI-6A | boulder | 18900 | 700 | 18000 | 600 | yes |
| LI-6B | boulder | 18300 | 500 | 17300 | 500 | yes |
| LI-7 | boulder | 18200 | 600 | 17200 | 500 | yes |
| LI-8 | boulder | 20900 | 700 | 20000 | 600 | yes |
| LI-9 | boulder | 14200 | 600 | 13300 | 500 | no |

Table 1 - Cont'd.

| Sample ID | Sample type | ¹⁰Be Age LSDn scaling (yrs) | ¹⁰Be age internal error LSDn Scaling (yrs) | ¹⁰Be Age St scaling (yrs) | ¹⁰Be age internal error St Scaling (yrs) | Included in landform age reported in Table 2? |
|---|--------------------|---|--|---|--|--|
| <i>Charlestown Moraine, Rhode Island</i> | | | | | | |
| GB2002-CH-1 | boulder | 17400 | 1600 | 16500 | 1500 | no |
| GB2002-CH-2 | boulder | 21800 | 800 | 21100 | 700 | yes |
| GB2002-CH-3 | boulder | 22200 | 1100 | 21500 | 1100 | yes |
| GB2002-CH-4 | boulder | 22500 | 800 | 21800 | 700 | yes |
| GB2002-CH-5 | boulder | 23700 | 1000 | 23100 | 1000 | yes |
| GB2002-CH-6 | boulder | 21900 | 1000 | 21100 | 1000 | yes |
| <i>Narragansett-Buzzards Bay Lobe</i> | | | | | | |
| <i>Congdon Hill Moraine</i> | | | | | | |
| GB2002-CO-1 | boulder | 21400 | 700 | 20600 | 700 | yes |
| GB2002-CO-2 | boulder | 20900 | 1000 | 20100 | 1000 | yes |
| GB2002-CO-3 | boulder | 20000 | 1200 | 19100 | 1100 | yes |
| <i>Hudson Lobe</i> | | | | | | |
| <i>Harbor Hill Moraine, Staten Island, NY</i> | | | | | | |
| SI-1 | boulder | 41600 | 2400 | 40700 | 2400 | n/a |
| SI-3 | boulder | 18900 | 2100 | 17800 | 2000 | n/a |

Table 1 - Cont'd.

| Sample ID | Sample type | ¹⁰ Be Age LSDn scaling (yrs) | ¹⁰ Be age internal error LSDn Scaling (yrs) | ¹⁰ Be Age St scaling (yrs) | ¹⁰ Be age internal error St Scaling (yrs) | Included in landform age reported in Table 2? |
|--|-------------|---|--|---------------------------------------|--|---|
| <i>Central Park, Manhattan, NY</i> | | | | | | |
| UDP-2 | bedrock | 25000 | 700 | 24200 | 700 | n/a |
| UDP-3 | bedrock | 23200 | 800 | 22300 | 800 | n/a |
| UDP-4 | boulder | 20000 | 700 | 19000 | 700 | n/a |
| <i>Lamont-Doherty Earth Observatory, Palisades, NY</i> | | | | | | |
| LDEO-1 | bedrock | 29000 | 1800 | 28200 | 1700 | n/a |
| <i>Harriman State Park, New York</i> | | | | | | |
| HSP-1 | boulder | 20600 | 700 | 19700 | 700 | yes |
| HSP-2a | boulder | 20300 | 700 | 19400 | 600 | yes |
| HSP-3 | boulder | 21500 | 700 | 20700 | 600 | yes |
| HSP-4 | boulder | 20300 | 800 | 19400 | 700 | yes |
| HSP-06-01 | boulder | 22800 | 800 | 22000 | 800 | yes |
| HSP-06-04 | boulder | 19100 | 700 | 18200 | 700 | yes |
| HSP-06-05 | boulder | 20200 | 600 | 19300 | 600 | yes |
| HSP-06-06 | boulder | 18700 | 700 | 17800 | 700 | yes |

Deleted: 2

Deleted: 8

Deleted: 4

Table 1 - Cont'd

| Sample ID | Sample type | ¹⁰ Be Age LSDn scaling (yrs) | ¹⁰ Be age internal error LSDn Scaling (yrs) | ¹⁰ Be Age St scaling (yrs) | ¹⁰ Be age internal error St Scaling (yrs) | Included in landform age reported in Table 2? |
|--------------------------|-------------|--|---|--|---|---|
| <i>Black Rock Forest</i> | | | | | | |
| BRF-1 | bedrock | 25000 | 700 | 24400 | 600 | n/a |
| BRF-2 | bedrock | 102400 | 2900 | 101400 | 2900 | n/a |
| BRF-3 | boulder | 22100 | 800 | 21500 | 800 | n/a |
| BRF-4 | boulder | 23700 | 800 | 23100 | 800 | n/a |
| BRF-19-01 | bedrock | 101100 | 3000 | 99900 | 3000 | n/a |

489

490

491 **5 Discussion**

492 The dataset of new and previously reported exposure ages spans the LGM (~26–19 ka), providing insight
 493 into the timing of the LIS maximum extent, the LGM duration, and implications for onset of initial retreat in southern
 494 New England and New York. We assess the exposure age chronology in more detail to establish an age for each ice
 495 limit, present estimates for average retreat rates through the study area and place the moraine chronology in a climatic
 496 context.

497 **5.1 Moraine ages**498 **5.1.1 Connecticut and Narragansett-Buzzards Bay Lobes**

499 The cosmogenic-nuclide chronology for the Connecticut and Narragansett-Buzzards Bay Lobes agrees with
 500 limiting age constraints from radiocarbon and glacial lake varves in the region (Figure 2; Figure 5), including for the
 501 timing of the LGM and onset of ice recession. The ¹⁰Be (26.5 ± 2.5 ka) and ²⁶Al ages (24.4 ± 2.1 ka) on the Martha's

502 Vineyard moraine agree within uncertainty with maximum-limiting radiocarbon ages in Port Washington, New York
503 Nantucket, MA, and near Boston, MA, as well as with OSL ages on Nantucket, which together suggest that the
504 southeastern LIS reached its maximum LGM extent by ~32.4–25.6 ka (Section 1.1.2; Balco et al., 2002; Oldale, 1982;
505 Rittenour, Stone and Mahan, 2012; Schafer and Hartshorn, 1965; Stone and Stone, 2019; Tucholke and Hollister,
506 1973). The Ledyard moraine (21.2 ± 0.7 ka; Balco and Schaefer, 2006) and Congdon Hill moraine (20.7 ± 0.7 ka), the
507 innermost recessional moraines discussed here, are slightly older than minimum-limiting ages for these moraines
508 placed by the varve sequences in the Quinnipiac Valley (18.9 ka; Ridge et al., 2012) and the Providence River (20.1
509 ka; Oakley and Boothroyd, 2013; Section 1.1.2).

Deleted:

510 Average exposure ages for each of the Connecticut and Narragansett-Buzzards Bay moraines are generally
511 in stratigraphic order, with the terminal limit being ~24.5–26.5 ka, the Roanoke Point-Charlestown-Buzzards Bay
512 limit being ~19.5–22.5 ka, and the inner limits in Connecticut and Rhode Island being ~20.5–21 ka (Table 2, Figure
513 6). Upon closer inspection, however, the average exposure ages on the Ronkonkoma moraine (20.8 ± 1.4), Roanoke
514 Point moraine (19.3 ± 1.1 ka) and Buzzards Bay moraine (21.2 ± 1.6 ka; Balco et al., 2002) are slightly younger than
515 those of stratigraphically equivalent (Charlestown) and/or inboard (Old Saybrook, Ledyard, and Congdon Hill)
516 moraines (Figure 6), although the age distributions on equivalent ice-margin limits overlap (Table 3; Figures 7). It is
517 not required that stratigraphically equivalent moraine segments are exactly the same age, as it is possible that the
518 timing of moraine emplacement was spatially variable across the region because of long occupation times and/or
519 asynchronous abandonment of the large moraine belts. Yet, it is expected that outboard moraines are older than those
520 inboard, so the apparent departure of average moraine age from stratigraphic ordering can be explained if i) the average
521 ages of the Connecticut and Rhode Island moraines are erroneously old due to nuclide inheritance, and/or ii) the
522 average ages from the Ronkonkoma, Roanoke Point and Buzzards Bay moraines are spuriously young because at least
523 some boulders were affected by postdepositional disturbance.

Deleted:

Deleted: due to

524 We find it unlikely that the boulders on the Charlestown, Old Saybrook, Ledyard and Congdon Hill moraines
525 contain significant inherited ^{10}Be . ^{10}Be , like most cosmogenic nuclides, is produced by neutron spallation and muon
526 interactions. Spallation dominates production at the Earth's surface and decreases rapidly with depth at an attenuation
527 length of ~160 g cm⁻² at mid-latitudes. Muon interactions account for ~2% of cosmogenic-nuclide production at the
528 Earth's surface but continue to tens of meters depth in rock, comprising the majority of ^{10}Be production below ~2 m
529 depth (Lal, 1991; Balco, 2017). Cosmogenic-nuclide inheritance is most often observed in places where subglacial
530 erosion is low, such as places with cold-based ice, and is generally more pervasive on bedrock surfaces than boulders
531 that have been entrained in ice (e.g., Stone et al., 2003; Young et al., 2016). The distribution of boulder exposure ages
532 on moraines where at least some boulders exhibit inheritance tend to skew old (Applegate et al., 2010), as is the case
533 on the Martha's Vineyard moraine. The distribution of exposure ages on the Connecticut and Rhode Island moraines,
534 however, are normal (Table 2; Figure 6), making the presence of inherited spallation-produced ^{10}Be highly unlikely
535 in the sampled boulders. Although muon-produced ^{10}Be accumulates slowly (< 0.1 atom g⁻¹ yr⁻¹), ^{10}Be builds to
536 measurable concentrations even at several meters depth when rock is exposed for the majority of a glacial cycle, as
537 are landscapes peripheral to the LGM ice sheets. Recent work demonstrates that moraine and erratic boulders near the
538 LGM limit may therefore contain several-thousand-years' worth of muon-produced ^{10}Be in excess of the deposition

Deleted: the boulders

543 age even when plucked from rock ~2–6 m below the formerly exposed surface (Briner et al., 2016b; Halsted et al.,
 544 2023). Yet, it is unlikely that all boulders on these moraines, which exhibit an abundance of large boulders (1–2 m;
 545 Figure 4), were sourced from the same depth in

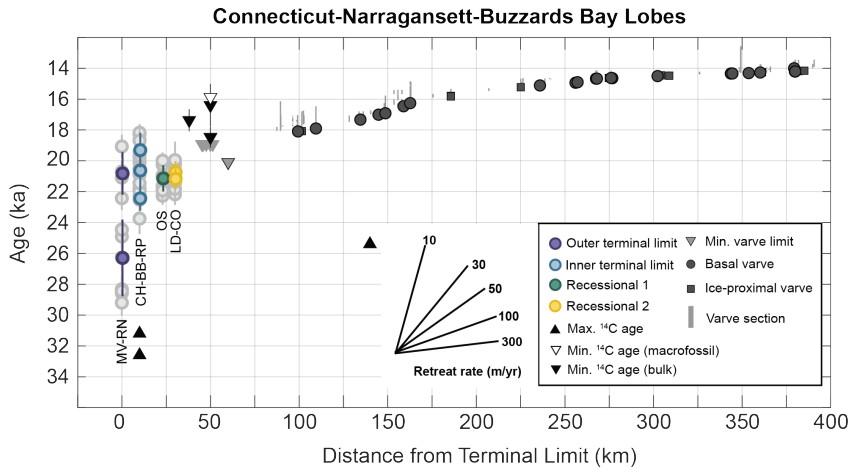


Figure 5 - Time distance diagram for the Connecticut-Narragansett-Buzzards Bay Lobes of the LIS based on the exposure age, radiocarbon, and varve chronologies. Only ¹⁰Be ages are shown for simplicity. Individual boulder ages are shown as light gray circles and average moraine ages are colored as in Figure 1. [Moraine names indicated below each limit in order of oldest to youngest. MV = Martha's Vineyard Moraine, RN = Ronkonkoma Moraine, CH = Charlestown Moraine, BB = Buzzard's Bay Moraine, RP = Roanoke Point Moraine, OS = Old Saybrook Moraine, LD = Ledyard Moraine, CO = Congdon Hill moraine.](#) Inset shows the slopes associated with various retreat rates.

546

Table 2 - Moraine ages and statistics.

| Moraine name | Distance from terminal moraine ¹ | Boulder count (samples excluded) | 1 σ error in | | 1 σ error in | | Coefficient of Variance (%) | Reduced χ^2 | Reference |
|--|--|---|--|---|---------------------------------------|--------------------------------------|-----------------------------------|-------------------|--------------------------------------|
| | | | LSDn Exposure age (yrs) ² | LSDn Exposure age (yr) ² | St Exposure age (yrs) ² | St Exposure age (yr) ² | | | |
| <i>Outer Terminal Limit</i> | | | | | | | | | |
| Budd Lake Moraine | 0 | 16 (0) | 25.7 | 2.0 | 24.9 | 2.1 | 8% | 6.14 | Corbett et al., 2017 |
| Ronkonkoma Moraine | 0 | 4 (0) | 20.8 | 1.4 | 19.9 | 1.4 | 7% | 3.36 | This study |
| Martha's Vineyard Moraine | 0 | 8 (4) | 25.4 | 2.5 | 24.9 | 2.6 | 8% | 6.09 | Balco et al., 2002 |
| <i>Inner Terminal Limit</i> | | | | | | | | | |
| Roanoke Point Moraine | 10 to 25 | 6 (1) | 19.3 | 1.1 | 18.3 | 1.1 | 6% | 3.33 | This study |
| Charlestown Moraine | 28 | 5 (1) | 22.4 | 0.8 | 21.7 | 0.8 | 4% | 0.68 | This study |
| Buzzards Bay Moraine | 8 to 30 | 10 (0) | 21.2 | 1.6 | 20.6 | 1.7 | 8% | 2.00 | Balco et al., 2002 |
| Roanoke Point- Charlestown- Buzzards Bay Combined | 8 to 30 | 12 (11) | 22.2 | 0.8 | 21.6 | 0.8 | 3% | 1.00 ⁴ | Balco et al., 2002 and this study |

Table 2 – Cont'd.

| Moraine name | Distance from terminal moraine ¹ | Boulder count (samples excluded) | 1σ error in | | 1σ error in | | Coefficient of Variance (%) | Reduced χ^2 | Reference |
|--|---|----------------------------------|--------------------------------------|-------------------------------------|------------------------------------|-----------------------------------|-----------------------------|------------------|--------------------------|
| | | | LSDn Exposure age (yrs) ² | LSDn Exposure age (yr) ² | St Exposure age (yrs) ² | St Exposure age (yr) ² | | | |
| <i>Recessional Limit 1</i> | | | | | | | | | |
| Old Saybrook Moraine | 35 to 43 | 7 (0) | 21.1 | 0.8 | 20.4 | 0.9 | 4% | 2.10 | Balco and Schaefer, 2006 |
| <i>Recessional Limit 2</i> | | | | | | | | | |
| Ledyard Moraine | 44 to 46 | 7 (0) | 21.2 | 0.7 | 20.4 | 0.7 | 3% | 1.21 | Balco and Schaefer, 2006 |
| Congdon Hill Moraine | 50 | 3 (0) | 20.7 | 0.7 | 19.9 | 0.7 | 3% | 0.59 | This study |
| Ledyard-Congdon Hill Combined | 44 to 50 | 10 (0) | 21.0 | 0.7 | 20.2 | 0.7 | 3% | 0.91 | This study |
| <i>Minimum Limit</i> | | | | | | | | | |
| Harriman State Park (ice-marginal deposit) | 40 to 50 | 8 (0) | 20.4 | 1.3 | 19.6 | 1.3 | 6% | 2.92 | This study |

¹Measured parallel to transect in Figure 1.

²All ages calculated using the primary production rate dataset of Borchers et al. (2016). Ages calculated using the NENA production rate dataset of Balco et al. (2009) shown in Table S3. All ages are from ¹⁰Be, except for on the Martha's Vineyard and Buzzards Bay moraines, for which ²⁶Al and ¹⁰Be measurements are reported and discussed in the original publication (Balco et al., 2002). ²⁶Al measurements are also reported for the Budd Lake moraine, but Corbett et al. (2017) do not discuss them because the ²⁷Al concentrations may have been underestimated for at least several samples, so the ²⁶Al exposure ages are not included in the moraine age calculation here.

³To calculate this moraine age and statistics, we: include the oldest boulder on the Roanoke Point moraine (LI-8); exclude the youngest four boulders on the Buzzards Bay moraine, as well as sample GB2002-BB2-29-1 because including it raises the reduced χ^2 value to ~40; and exclude the youngest boulder on the Charlestown moraine. Including sample GB2002-BB2-29-1 in the average does not change the rounded exposure age reported here.

⁴Sample GB2002-BB2-29-1 is excluded from the average because including it raises the reduced χ^2 value to ~40. Including this sample does not affect the rounded exposure age reported here.

549 rock. If some boulders were sourced above this zone (~2–6 m), we would expect to see more scatter in these exposure-
 550 age datasets; if at least some boulders were sourced below these depths, inherited muon-produced ¹⁰Be in those
 551 samples would be negligible, but together with boulders sourced from above or within this zone, the age distribution
 552 would still skew old (Briner et al., 2016b). The morphology of the moraines along with the uniform age distributions
 553 and lack of scatter suggest that the exposure ages on these moraines represent their true deposition age within
 554 uncertainties (Table 2).
 555

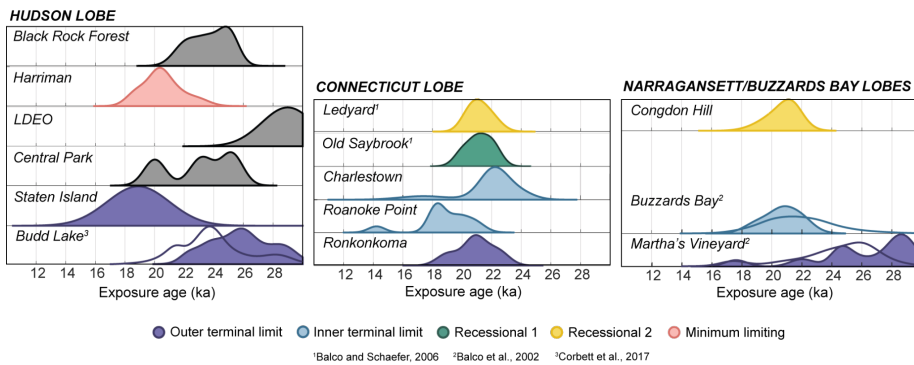


Figure 6 - Camel plots for moraine exposure ages grouped by LIS lobe. Colors are the same as Figure 1. Filled camel plots show the relative probability distribution for the ¹⁰Be age of the moraine and open camel plots show the probability distribution for the ²⁶Al age. Note the normal age distributions of the Ledyard, Old Saybrook, Charlestown and Harriman moraine boulders compared to the age distribution of the Martha's Vineyard moraine, which likely includes both postdepositional disturbance (young outliers) and inheritance (old outliers). See Tables 1 and S2 for outlier identification.

556
 557 Instead, the preponderance of boulders with ages that may be slightly younger than the true emplacement age
 558 on the Ronkonkoma, Roanoke Point and Buzzards Bay moraines is most likely explained by a small degree of
 559 postdepositional disturbance. These large end moraines have broad, relatively flat crests comprising a complex of
 560 moraine ridges with kettle and kame topography, indicating that the moraines were almost certainly ice cored after
 561 the LIS abandoned these positions and underwent post-emplacement settling. In addition, agricultural disturbances or
 562 other human-induced environmental modification may have contributed to the movement or exhumation of boulders
 563 on these moraines. Balco (2011) recognized that the Buzzards Bay ¹⁰Be and ²⁶Al measurements, independent analyses
 564 that should be uncorrelated if scatter in the dataset is due to measurement error alone, were in fact correlated unless
 565 the four youngest ages are discarded, indicating the presence of geologic scatter. A moderate relationship between
 566 boulder height and exposure age ($r^2 = 0.36$) suggests that sediment or snow cover is a likely source of this scatter
 567 (Balco, 2011). Discarding the four youngest ages gives an average age of 22.1 ± 0.6 ka for the Buzzard's Bay moraine.
 568 The geomorphic setting of the boulders sampled on the Ronkonkoma and Roanoke Point moraines indicates a similar
 569 role for post depositional disturbance as on the Buzzards Bay moraine. Boulders suitable for exposure-age dating were

Deleted: and

Deleted: at

Deleted: reflecting

Deleted: measurements

Deleted: the

575 difficult to locate on the Ronkonkoma moraine as the moraine comprises mostly sandy outwash till, which may have
 576 been affected by LIS meltwater as it occupied a more northern position (Section 2.1.1). Samples on the Roanoke Point
 577 moraine generally came from large boulders (>1 m) situated in local depressions and/or inboard of the moraine crest
 578 (Section 2.1.1; Figure S1), so may have been

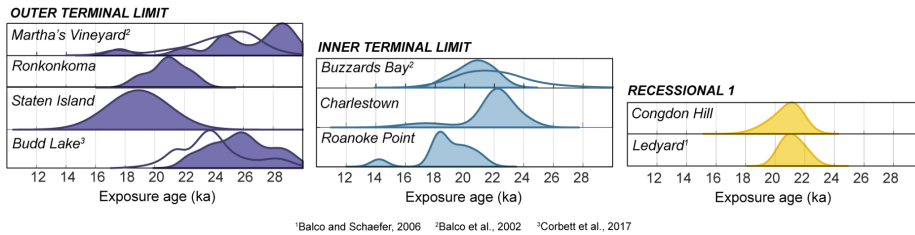


Figure 7 - Camel plots for moraine exposure ages grouped by ice-margin limit. Colors are the same as Figure 1 and only ice-margin limits with more than one moraine are shown. Filled camel plots show the probability distribution for the ^{10}Be age of the moraine and open camel plots show the probability distribution for the ^{26}Al age.

579 subjected to hillslope processes and/or been encased in stagnant ice even after initial moraine abandonment. It is also
 580 possible these boulders were affected by human modification of the environment. In contrast, the two oldest boulders
 581 on the Roanoke Point moraine (LI-1, 20.1 ± 1.0 ka and LI-8, 20.9 ± 0.7 ka), while also located slightly inboard of the
 582 moraine crest, rest on local highs where they may have been more stable (Figure S1).

583 Given the geomorphic context of the Ronkonkoma, Roanoke Point and Buzzards Bay samples, it is possible
 584 that averaging the exposure ages of all boulders from these moraines slightly underestimates the true emplacement
 585 age. On the other hand, the oldest exposure ages from the Ronkonkoma, Roanoke Point and Buzzards Bay moraines
 586 generally overlap with the age distributions of stratigraphically equivalent or inboard moraines (Figures 6 and 7),
 587 suggesting that the oldest ages of the main population are a better estimate of the emplacement age than the average
 588 age. The wide age distribution on the Martha's Vineyard moraine, which includes young ages (~17 ka), is also
 589 consistent with the interpretation that at least parts of the large, hummocky end moraines are affected by
 590 postdepositional disturbance (Figures 6 and 7; Balco et al., 2002). The Martha's Vineyard age distribution also
 591 includes older ages indicative of inheritance, which is to be expected given that the first advance of the LIS to its
 592 terminal position likely remobilized boulders exposed during the preceding interglacial period and prior to expansion
 593 to the southernmost limits.

594 Guided by these arguments, we present emplacement ages for the moraines deposited by the Connecticut and
 595 Narragansett-Buzzards Bay Lobes of the LIS, recognizing that they are differentially affected by postdepositional
 596 disturbance and nuclide inheritance. For the Martha's Vineyard moraine, we take the average of the ^{10}Be and ^{26}Al
 597 ages of the main population, which yields an age of 25.4 ± 2.5 ka (Balco et al., 2002). The oldest age on the
 598 Ronkonkoma moraine (22.4 ± 0.8 ka) is probably closer to the true deposition age than the average (20.8 ± 1.4 ka),
 599 although they do overlap within uncertainty. For the Roanoke Point-Charlestown-Buzzards Bay limit, we take the
 600 average age of the Buzzards Bay boulders, excluding the four youngest (Balco, 2011); the oldest boulder on Roanoke

601 Point moraine; and the main age population on Charlestown moraine, which gives an age for this limit of 22.2 ± 0.8
602 ka (Table 2). We take the average age of the Old Saybrook moraine to represent its true deposition age (21.1 ± 0.8 ka;
603 Balco and Schaefer, 2006). The Ledyard Moraine (Balco and Schaefer, 2006) and Congdon Hill moraines are
604 stratigraphically correlated, and their exposure ages agree within measurement uncertainty (reduced X^2 of combined
605 population = 1), so we combine their exposure ages to represent the true age of the limit (21.0 ± 0.8 ka; Table 2).

606

607 5.1.2 Hudson Lobe

608 The exposure-age, radiocarbon, and OSL chronologies for LIS retreat in the Hudson River Valley are
609 generally consistent, although some conflicts remain (Figures 2 and 3). As described in detail in previous studies, the
610 cosmogenic exposure ages at the Budd Lake moraine (25.7 ± 2.0 ka; Corbett et al., 2017) agree within uncertainty
611 with the maximum-limiting radiocarbon ages in Long Island and in Manhattan (26.1–25.8 ka; Schuldenrein and
612 Aiuvalasit, 2011; Sirkin and Stuckenrath, 1980), maximum-limiting OSL ages at Jones Point, New York (25.3 ± 7.4
613 ka; Gorokhovitch et al., 2018), and a minimum-limiting radiocarbon age of 24.2 ± 1.1 ka in a concretion of postglacial
614 lake sediment just south of the terminal moraine (Stanford et al., 2021). The Budd Lake moraine exposure ages also
615 overlap with the age distribution on the Martha's Vineyard moraine (Section 5.1.1; Balco et al., 2002; Corbett et al.,
616 2017). Two boulders on the Harbor Hill moraine on Staten Island, New York, have disparate ages (18.9 ka and 41.6
617 ka; Table 1), similar to the distribution of ages on Martha's Vineyard, which is affected by inheritance and
618 postdepositional disturbance (Figure S3). Therefore, we cannot disprove the hypothesis that the moraine on Staten
619 Island was deposited at the same time as the Budd Lake, Ronkonkoma, and Martha's Vineyard moraines, as the
620 stratigraphic correlation suggests.

621 Exposure ages on bedrock surfaces in New York City and the lower Hudson Valley are consistently older
622 than co-located boulders. Two bedrock ages (25.0 ± 0.7 and 23.2 ± 0.8 ka) in Central Park, New York are older than
623 a nearby boulder (20.0 ± 0.7 ka); a single bedrock sample at the Lamont-Doherty Earth Observatory dates to $29.0 \pm$
624 1.8 ka; and at Black Rock Forest three bedrock ages (one of 25.0 ± 0.7 ka and two of $\sim 100 \pm 3$ ka) are significantly
625 older than two boulder samples from the same location (22.1 ± 0.8 ka and 23.7 ± 0.8 ka; Figure 3). Furthermore, the
626 bedrock ages at LDEO and Black Rock Forest are older than nearby radiocarbon ages that suggest the ice margin did
627 not retreat north of LDEO until ~ 22.5 ka and north of Black Rock Forest until ~ 20 – 19 ka (Stanford et al., 2021). The
628 fact that bedrock exposure ages significantly pre-date nearby boulders and radiocarbon ages indicates cosmogenic-
629 nuclide inheritance, implying that erosion beneath the LIS at these sampling locations was insufficient to remove ^{10}Be
630 to background levels in bedrock, perhaps because ice was thin and slow-flowing or because of short ice-cover
631 durations, or both. The three erratic boulder ages in our Hudson Valley transect do not exhibit a clear trend with
632 distance from the terminal moraine, where the age in Central Park (20.0 ka) is significantly younger than two ages at
633 Black Rock Forest (22.1 ka and 23.7 ka), ~ 80 km to the north. Given the presence of inheritance in the bedrock ages
634 and lack of spatial trend in the boulder ages in the Hudson Valley, we exclude these ages from further discussion here,
635 and identify additional collection of bedrock and boulder samples in this region as a potential direction for future
636 work.

Deleted:

Deleted:

Deleted:

Deleted: .²

641 The average age of the ice-marginal deposit in Harriman State Park (20.4 ± 1.3 ka; Figures 3 and 6) is
642 consistent with the minimum limiting age of the varve sequence at Haverstraw, New York (18.9 ka; Ridge et al.,
643 2012), situated a similar distance from the terminal moraine, and is older than the youngest boulder age on a former
644 nunatak at Peekamoose Mountain (18.6 ka) ~80 km to the north (Halsted et al., 2022). Finally, the average ^{10}Be age
645 of the Harriman State Park boulders of 20.4 ± 1.3 ka is slightly younger than the Ledyard moraine exposure age (21.2
646 ± 0.7 ka), although the ages overlap within 1σ uncertainty, supporting the correlation of the Augusta and Sussex limits
647 in northern New Jersey with the Connecticut moraines (Section 1.1.1; Stone et al., 2005). This interpretation, however,
648 remains in disagreement with recent work that suggests all three moraines in northern New Jersey are ~23.5, and that
649 the Connecticut moraines may instead correlate with the Pellets Island and New Hampton moraines to the north
650 (Figure 1; Stanford et al., 2021). Nevertheless, the age of the Harriman State Park ice-marginal deposit agrees with
651 the majority of bulk radiocarbon ages in northern New Jersey as summarized by Stanford et al. (2021; Figure 2).

652

653 5.1.3 Summary of regional deglaciation chronology

654 To summarize the exposure-age chronology, the southeastern LIS occupied the terminal complex from ~26
655 to 22 ka, with the outermost moraine ridges dating to 25.4 ± 2.5 ka at Martha's Vineyard (Balco et al., 2002) and 25.7
656 ± 2.0 ka at Budd Lake in New Jersey (Corbett et al., 2017). The inner terminal limit at Roanoke Point-Charlestown-
657 Buzzards Bay, located 10–30 km north of the outer terminal ridge, dates to 22.2 ± 0.8 ka. The fact that the innermost
658 portion of the terminal complex is nearly 4 kyr younger than the outermost ridges could represent slow, secular retreat
659 of the ice margin through this period, or the position of the moraines could reflect fluctuations of the ice margin during
660 the LGM, with the culmination of readvances occurring within the terminal moraine belt. We prefer the latter
661 interpretation given that the geomorphology and sedimentology of these moraines indicate construction by an
662 advancing LIS and note that it is unknown how far ice retreated between readvances (Boothroyd et al., 1998; Oldale
663 and O'Hara, 1984; Sections 1.1.1 and 2.2.1).

664 Irreversible deglaciation began with the abandonment of the inner terminal moraine at ~22 ka, after which
665 the ice margin did not reoccupy the terminal complex. Ice-margin positions in southern Connecticut and Rhode Island
666 are marked by smaller, discontinuous, boulder-rich moraines interpreted as recessional limits deposited during brief
667 re-advances or standstills (Stone et al., 2005). The Old Saybrook moraine, ~40 km inboard of the outer terminal limit,
668 is 21.1 ± 0.8 ka (Balco and Schaefer, 2006), and the Ledyard-Congdon Hill limit ~45–50 km north of the outer terminal
669 ridge, is 21.0 ± 0.8 ka. The ice-marginal deposit in Harriman State Park, which is morpho-stratigraphically inboard of
670 the Ledyard-Congdon Hill limit, is 20.4 ± 1.3 ka. Therefore, the exposure-age chronology presented here spans ~25.5–
671 20.5 ka. The LIS then retreated to the spillway for glacial Lake Hitchcock in Rocky Hill, CT, ~90–100 km north of
672 the outer terminal moraine, by ~18.2 ka (Ridge et al., 2012). A lack of extensive end moraine deposits between the
673 Ledyard-Congdon Hill limit and Rocky Hill, CT signals a shift to more continuous retreat north of our study area.

674 The positions of the moraines represent net changes in LIS extent from which we estimate average retreat
675 rates, calculated using the maximum and minimum distance between moraine ridges measured parallel to the transect
676 in Figure 1, divided by the difference in age established for each limit (Table 2; Figure 8). Although these rates
677 represent overall northward movement of the ice-margin position (i.e., retreat), they integrate periods of retreat,

Deleted:

Deleted: bedrock

Deleted: Mt.

681 advance, and minimal change given that the moraines themselves were formed during readvances or standstills. In
682 this context, the terminal moraine belt represents several ice-margin fluctuations, with the rate of change in ice-margin
683 position from the outer terminal to inner terminal limit averaging $<5\text{--}10\text{ m yr}^{-1}$. Ice then retreated from the inner
684 terminal position to the Ledyard-Congdon Hill limit at an average rate of $\sim 10\text{--}20\text{ m yr}^{-1}$. Further retreat through
685 southern Connecticut and Rhode Island was interrupted by several standstills or re-advances during which additional
686 recessional moraines, including the Old Saybrook moraine, were deposited. After abandoning of the Old Saybrook
687 moraine, the LIS withdrew to Rocky Hill, Connecticut, at an average rate of $\sim 15\text{--}25\text{ m yr}^{-1}$ (Ridge et al., 2012). North
688 of our study area, the NAVC reveals moderate retreat rates of $\sim 30\text{--}100\text{ m yr}^{-1}$ during Heinrich Stadial 1 ($\sim 18\text{--}15\text{ ka}$),
689 with an abrupt increase in retreat rate to $>300\text{ m yr}^{-1}$ at the onset of the Bølling-Allerød $\sim 15\text{ ka}$ (Figure 8; Ridge et al.,
690 2012). [A prominent set of moraines along coastal Maine also may suggest slow but steady net retreat during the latter](#)
691 [part of Heinrich Stadial 1 \(Borns et al., 2004; Kaplan, 1999; Hall et al., 2017\)](#). Similar retreat rates ($100\text{--}300\text{ m yr}^{-1}$)
692 are implied by DeGeer moraines interpreted to mark the annual retreat of the ice margin in southern New Hampshire,
693 Maine and Atlantic Canada around 15 ka (Sinclair et al., 2018; Todd et al., 2007; Wroblewski, 2020). Cosmogenic-
694 exposure ages from former nunataks that serve as “dipsticks” for LIS thickness also show moderate thinning through
695 HS1 followed by rapid LIS thinning at the onset of the Bølling (Halsted et al., 2022).

696 The regional moraine chronology is remarkably consistent with the varve chronologies, OSL ages, and many
697 of the radiocarbon ages throughout the region, as discussed above (Figure 5). Yet, the absence of radiocarbon ages on
698 plant macrofossils between ~ 26 and 16 ka remains unresolved (Peteet et al., 2012; Figures 2, 3, and 5). This absence
699 could potentially be explained by i) poor preservation of macrofossils from this time period, ii) landscape instability
700 and/or sparse vegetation [in the study area](#) during the LGM and early deglaciation, iii) the delay of widespread organic
701 sediment deposition until beaver colonies expanded into the region, damming lakes and wetlands (Kaye, 1962), iv)
702 the predominance of seepage ponds in permeable sand and other ice proximal coarse deposits on end moraines which
703 are susceptible to periodic drainage, v) difficulty in coring to the till contact [and/or stratigraphic disturbance](#) in lake
704 sediment affected by postglacial permafrost (Prince et al., 2024) and/or vi) persistent lake ice during HS1 ($\sim 18\text{--}15\text{ ka}$)
705 [spring or](#) summers that precluded organic lake sedimentation. Further discussion of the $\sim 10\text{ kyr}$ gap between the
706 moraine emplacement age indicated by the exposure-age chronology and the widespread occurrence of radiocarbon-
707 dated organic material 16 ka is beyond the scope of this paper.

708

Deleted: .

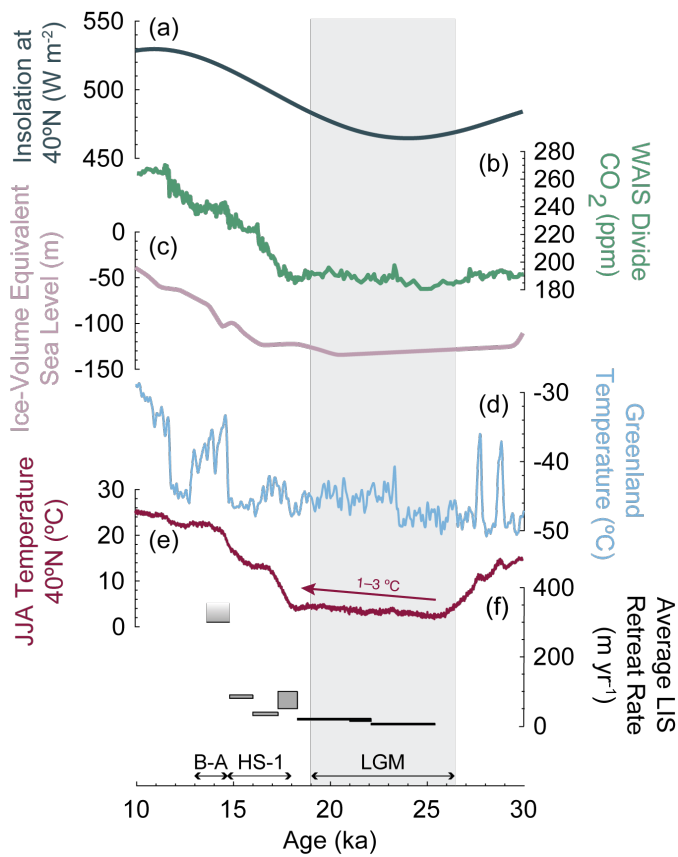


Figure 8 - LIS ice-margin chronology and average retreat rates compared to other climate parameters and records. a) June 21st insolation at 40°N (Laskar et al., 2004). b) compilation of atmospheric CO₂ measured in Antarctic ice cores (Bereiter et al., 2014; Monnin et al., 2001, 2004; Marcott et al., 2014; Ahn et al., 2014). c) global ice-volume equivalent sea-level (Lambeck et al., 2014). d) Greenland mean-annual temperature reconstruction based on $\delta^{15}\text{N}-\text{N}_2$ in the NGRIP ice core (Kindler et al., 2014). e) time series of summer (June, July and August) surface temperatures modeled using the Had3CMB-M2.1 coupled general circulation model that incorporates Dansgaard-Oeschger and Heinrich events (Armstrong et al., 2019). The time series shown here is for 40°N, 75.5°W, ~50 km south of the LGM limit in a part of northern New Jersey that was not covered by ice during the LGM. f) Average LIS retreat rates. Rates shown in black are from this study and those shown in gray are from Ridge et al. (2012), with the faded gray bar indicating a minimum retreat rate of 300 m yr⁻¹. The range of average retreat rates are calculated using the maximum and minimum distance between moraine ridges measured parallel to the transect in Figure 1, divided by the difference in age established for each limit (Table 2). Vertical gray bar in the background denotes the LGM timing from 26.5–19 ka (Clark et al., 2009). Heinrich Stadial 1 (HS-1; ~18–15 ka) and Bolling-Allerød (B-A; ~15–13 ka) are periods of abrupt climate change discussed in the text.

711 **5.2 Climatic context for initial LIS retreat**

712 The exposure-age-derived moraine chronology suggests that the LIS occupied the terminal moraine complex
713 between ~26 and 22 ka and remained within 50 km of its southernmost position until ~21 ka (Balco et al., 2002; Balco
714 and Schaefer, 2006; Corbett et al., 2017). The moraines discussed here therefore span the canonical LGM and global
715 sea-level lowstand (26.5–19.0 ka; Lambeck et al., 2014; Clarke et al., 2009) and coincide with a local insolation
716 minimum at ~24 ka (Figure 8; Laskar et al., 2004). Furthermore, the timing of terminal moraine occupation from ~26
717 to 22 ka is similar to that of other LIS sectors to the west, as well as other ice sheets fringing the North Atlantic (Balco
718 et al., 2002; Corbett et al., 2017; Section 5.1.3). For example, exposure and radiocarbon ages indicate the glacial
719 maximum occurred in Wisconsin and Illinois by ~24–23 ka (Ullman et al., 2015; Currey and Petras, 2011) and a
720 minimum limiting radiocarbon age on the terminal moraine of the Miami-Scioto lobe in Indiana and Ohio indicates
721 retreat began sometime before 22.4 ka (Glover et al., 2011). Parts of the British-Irish Ice Sheet began to retreat by
722 ~30–26 ka (Clark et al., 2022) and the Scandinavian ice sheet on Andøya, Norway, fluctuated near its maximum extent
723 from ~26–22 ka (Vorren et al., 2015). Retreat from the terminal moraine complex ~22 ka is consistent with ice-sheet
724 mass balance modeling, which indicates that the moderate increase in local summer insolation beginning ~24 ka may
725 have driven initial LIS margin retreat from its southernmost position (Ullman et al., 2015). We emphasize, however,
726 that the ~50 km of net change in ice-margin position from the outer terminal moraine to the Ledyard-Congdon Hill
727 limit **is modest in the context of the entire ice sheet. This distance** represents <2% of total LIS margin change
728 **considering** that the former LIS is now restricted to the Barnes and Penny Ice Caps on the central Baffin plateau ~3000
729 km to the north (Dalton et al., 2020; Dyke, 2004; Hooke, 1976; Hooke and Clausen, 1982; Refsnider et al., 2014), **and**
730 **likely significantly less when expressed volumetrically since the LIS would have been thinner at its margin than**
731 **towards the centre of the ice sheet (e.g., Stokes et al., 2012).**

Deleted:

Deleted: given

Deleted: .

732 The chronology supports the hypothesis that initial LIS retreat, albeit slow (<5–25 m yr⁻¹; Section 5.1.3),
733 began when cold mean-annual temperatures persisted in the Arctic (Kindler et al., 2014) and atmospheric CO₂
734 concentrations remained at glacial values (Figure 8; Denton et al., 2010; Marcott et al., 2014; Raymo, 1997; Ullman
735 et al., 2015; Figure 8). Yet, insight into local summer conditions may provide additional context for the relatively
736 modest LIS retreat during the LGM. Ridge et al. (2012) established a strong relationship, especially after ~15 ka,
737 between LIS retreat rates, the Greenland temperature record, and local summer conditions as recorded by varve
738 thickness, which is largely controlled by LIS meltwater production. In the absence of varve thickness as a proxy for
739 summer climate conditions prior to ~18 ka, we use output from a recent model reconstruction of Northern Hemisphere
740 land surface air temperatures over the last 60 kyr to estimate changes in summer temperature coincident with the
741 moraine chronology discussed here (Figure 8; Armstrong et al., 2019). Modeled terrestrial summer temperature at
742 40°N, 75.5°W, ~50 km south of the LGM limit in northern New Jersey, exhibits a slow but steady increase of ~1–3°C
743 from 26–19 ka and sharp rise beginning at ~18 ka (Figure 8; Armstrong et al., 2019). The pattern of modeled summer
744 temperature change bears striking resemblance to the slow net LIS retreat (<5–25 m yr⁻¹) from ~26–21 ka as indicated
745 by the moraine record, and acceleration of ice-margin retreat after ~18 ka (30–>300 m yr⁻¹), as observed in the NAVC
746 (Ridge et al., 2012). We therefore suggest that the relationship between LIS behavior, including relative ice margin

750 positions, and summer conditions observed by Ridge et al. (2012) extends to the LGM. Altogether, the moraine record
751 in southern New England and New York records LIS fluctuations and modest retreat through the LGM, consistent
752 with a slight increase in modeled summer temperature during that interval, with deglaciation accelerating after 18 ka
753 alongside the rise in atmospheric CO₂ and the onset of Termination 1.

754 **6 Conclusions**

- 755 • The exposure-age chronology in southern New England and New York agrees with established regional
756 stratigraphic relationships and independent age constraints from radiocarbon and glacial lake varves.
- 757 • The few inconsistencies in the regional exposure-age dataset can be explained by systematic geologic scatter
758 where i) bedrock samples are affected by nuclide inheritance, ii) the outermost LGM moraine exhibits
759 inheritance on some boulders, and iii) some exposure ages on large unconsolidated landforms that may have
760 experienced extended permafrost conditions are affected by postdepositional disturbance while more stable
761 landforms are not. Also, we cannot rule out that the boulders with the youngest exposure were affected by
762 agricultural practices and other human activities.
- 763 • Considering the impact of this geologic scatter, we conclude that the LIS occupied the terminal complex from
764 ~26 ka to ~22 ka (Balco, 2011; Balco et al., 2002). We date several inboard moraines and other recessional
765 deposits to ~21–20.5 ka (Balco and Schaefer, 2006).
- 766 • The moraine chronology for the southeastern LIS spans ~26–21 ka, which is consistent with the canonical
767 LGM and sea-level lowstand, full glacial conditions in Greenland, and is broadly coincident with a minimum
768 in local summer insolation.
- 769 • Average LIS retreat rates from ~26–18 ka (<5 to 25 m yr⁻¹) are consistent with slight warming (1–3°C) in
770 modeled local summer temperature through the LGM, but were slower than at any point during Termination
771 1 (>30 to >300 m yr⁻¹; Ridge et al., 2012), although this does not account for any distance covered by the
772 readvance or stillstand, if significant. Hence, we conclude that the major pulse of deglaciation and marked
773 recession did not begin until after ~18 ka, when a dramatic rise in atmospheric CO₂ signals the onset of
774 Termination 1.

776 **Data Availability**

777 All analytical information associated with new cosmogenic-nuclide measurements appear in the tables and
778 Supplement. Analytical information, with additional sample documentation and photographs, is also available in the
779 ICED:LAURENTIDE online database (<https://version2.ice-d.org/laurentide/publication/1187/>, Balco, 2024).

Deleted: <https://version2.ice-d.org/laurentide/>,

781 **Competing Interests**

782 The contact author has declared that none of the authors has any competing interests.

784 **Acknowledgements**

785 We thank the many people who helped support this work in the lab and field, including Sidney Hemming, as well as
786 Mikah McCabe and Rebecca Steinberg who helped collect and process samples as interns in the Lamont-Doherty
787 Earth Observatory Summer Intern Program. We are immensely grateful to the late Jon Boothroyd of the University
788 of Rhode Island and the late Gil Hanson of Stony Brook University for sharing their expertise in the regional
789 stratigraphy and geomorphology. This work was supported in part by the National Science Foundation Graduate
790 Research Fellowship under grant no. DGE 2036197 to Allie Balter-Kennedy. Joerg Schaefer acknowledges support
791 by the Vetlesen Foundation and the LDEO Climate Center.

792 **References**

- 793 Andersen, K. K., Svensson, A., Johnsen, S. J., Rasmussen, S. O., Bigler, M., Röthlisberger, R., Ruth, U., Siggaard-
794 Andersen, M.-L., Steffensen, J. P., Dahl-Jensen, D., Vinther, B. M., and Clausen, H. B.: The Greenland Ice
795 Core Chronology 2005, 15–42ka. Part 1: constructing the time scale, *Quaternary Sci Rev*, 25, 3246–3257,
796 <https://doi.org/10.1016/j.quascirev.2006.08.002>, 2006.
- 797 Antevs, E.: The last glaciation, with special reference to the ice sheet in northeastern North America, *American*
798 *Geographical Society Research Series*, 292, 1928.
- 799 Antevs, E.: The recession of the last ice sheet in New England. *American Geographical Society Research Series* 11
800 (with a preface and contributions by J. W. Goldthwait) 120, 1922.
- 801 Applegate, P. J., Urban, N. M., Keller, K., Lowell, T. V., Laabs, B. J. C., Kelly, M. A., and Alley, R. B.: Improved
802 moraine age interpretations through explicit matching of geomorphic process models to cosmogenic nuclide
803 measurements from single landforms, *Quaternary Res*, 77, 293–304,
804 <https://doi.org/10.1016/j.yqres.2011.12.002>, 2012.
- 805 Applegate, P. J., Urban, N. M., Laabs, B. J. C., Keller, K., and Alley, R. B.: Modeling the statistical distributions of
806 cosmogenic exposure dates from moraines, *Geosci Model Dev*, 3, 293–307, [https://doi.org/10.5194/gmd-3-](https://doi.org/10.5194/gmd-3-293-2010)
807 293-2010, 2010.
- 808 Armstrong, E., Hopcroft, P. O., and Valdes, P. J.: A simulated Northern Hemisphere terrestrial climate dataset for the
809 past 60,000 years, *Sci Data*, 6, 265, <https://doi.org/10.1038/s41597-019-0277-1>, 2019.
- 810 Balco, G. and Schaefer, J. M.: Cosmogenic-nuclide and varve chronologies for the deglaciation of southern New
811 England, *Quat Geochronol*, 1, 15–28, <https://doi.org/10.1016/j.quageo.2006.06.014>, 2006.
- 812 Balco, G., Briner, J., Finkel, R. C., Rayburn, J. A., Ridge, J. C., and Schaefer, J. M.: Regional beryllium-10 production
813 rate calibration for late-glacial northeastern North America, *Quat Geochronol*, 4, 93–107,
814 <https://doi.org/10.1016/j.quageo.2008.09.001>, 2009.
- 815 Balco, G., DeJong, B. D., Ridge, J. C., Bierman, P. R., and Rood, D. H.: Atmospherically produced beryllium-10 in
816 annually laminated late-glacial sediments of the North American Varve Chronology, *Geochronology*, 3, 1–
817 33, <https://doi.org/10.5194/gchron-3-1-2021>, 2021.
- 818 Balco, G., Stone, J. O. H., Porter, S. C., and Caffee, M. W.: Cosmogenic-nuclide ages for New England coastal
819 moraines, Martha's Vineyard and Cape Cod, Massachusetts, USA, *Quaternary Sci Rev*, 21, 2127–2135,
820 [https://doi.org/10.1016/s0277-3791\(02\)00085-9](https://doi.org/10.1016/s0277-3791(02)00085-9), 2002.
- 821 Balco, G., Stone, J. O., Lifton, N. A., and Dunai, T. J.: A complete and easily accessible means of calculating surface
822 exposure ages or erosion rates from ^{10}Be and ^{26}Al measurements, *Quat Geochronol*, 3, 174–195,
823 <https://doi.org/10.1016/j.quageo.2007.12.001>, 2008.
- 824 Balco, G.: Contributions and unrealized potential contributions of cosmogenic-nuclide exposure dating to glacier
825 chronology, 1990–2010, *Quaternary Sci Rev*, 30, 3–27, <https://doi.org/10.1016/j.quascirev.2010.11.003>,
826 2011.

827 Balco, G.: ICE-D:LAURENTIDE, available at: <https://version2.ice-d.org/laurentide/publication/1187/>, last access: 11,
828 July, 2024.

829 Balco, G.: Production rate calculations for cosmic-ray-muon-produced ^{10}Be and ^{26}Al benchmarked against
830 geological calibration data, *Quat. Geochronol.*, 39, 150–173, <https://doi.org/10.1016/j.quageo.2017.02.001>,
831 2017.

832 Barker, S. and Knorr, G.: Millennial scale feedbacks determine the shape and rapidity of glacial termination, *Nat*
833 *Commun*, 12, 2273, <https://doi.org/10.1038/s41467-021-22388-6>, 2021.

834 Barker, S., Diz, P., Vautravers, M. J., Pike, J., Knorr, G., Hall, I. R., and Broecker, W. S.: Interhemispheric Atlantic
835 seesaw response during the last deglaciation, *Nature*, 457, 1097–1102, <https://doi.org/10.1038/nature07770>,
836 2009.

837 Boothroyd, J. C., and Sirkin, L.: The Quaternary geology of Block Island and adjacent regions, in Paton, P., Gould,
838 L. I., August, P. V., and Frost, A. O., eds., *The Ecology of Block Island: Kingston, Rhode Island*, Rhode
839 Island Natural History Survey, p. 13-27, 2002.

840 Boothroyd, J. C., McCandless, S. J., and Dowling, M. J.: Quaternary Geologic Map of Rhode Island: Rhode Island
841 Geological Survey STATEMAP Program, scale scale: 1:100,000.
842 http://geothermal.isgs.illinois.edu/aasggeothermal/rigs/map/RI_Quaternary_Geology_100K.zip, 2003.

843 Boothroyd, J.C., Freedman, J.H., Brenner, H.B., Stone, J.R.: The Glacial Geology of Southern and Central Rhode
844 Island, in: Murray, D.P. (Ed.), *Guidebook to Field Trips in Rhode Island and Adjacent Regions of*
845 *Connecticut and Massachusetts*. Presented at the New England Intercollegiate Geological Conference: 90th
846 Annual Meeting, Kingston, Rhode Island, pp. C5-1:25., 1998.

847 Borchers, B., Marrero, S., Balco, G., Caffee, M., Goehring, B., Lifton, N., Nishiizumi, K., Phillips, F., Schaefer, J.,
848 and Stone, J.: Geological calibration of spallation production rates in the CRONUS-Earth project, *Quat*
849 *Geochronol*, 31, 188–198, <https://doi.org/10.1016/j.quageo.2015.01.009>, 2016.

850 [Borns, H. W., Doner, L. A., Dorion, C. C., Jacobson, G. L., Kaplan, M. R., Kreutz, K. J., Lowell, T. V., Thompson,](#)
851 [W. B., and Weddle, T. K.: The deglaciation of Maine, U.S.A., *Dev. Quat. Sci.*, 2, 89–109,](#)
852 [https://doi.org/10.1016/s1571-0866\(04\)80190-8](https://doi.org/10.1016/s1571-0866(04)80190-8), 2004.

853 Briner, J. P., Goehring, B. M., Mangerud, J., and Svendsen, J. I.: The deep accumulation of ^{10}Be at Utsira,
854 southwestern Norway: Implications for cosmogenic nuclide exposure dating in peripheral ice sheet
855 landscapes, *Geophys Res Lett*, 43, 9121–9129, <https://doi.org/10.1002/2016gl070100>, 2016.

856 Briner, J. P., McKay, N. P., Axford, Y., Bennike, O., Bradley, R. S., Vernal, A. de, Fisher, D., Francus, P., Fréchette,
857 B., Gajewski, K., Jennings, A., Kaufman, D. S., Miller, G., Rouston, C., and Wagner, B.: Holocene climate
858 change in Arctic Canada and Greenland, *Quaternary Sci Rev*, 147, 340–364,
859 <https://doi.org/10.1016/j.quascirev.2016.02.010>, 2016.

860 Brock, P. C. and Brock, P. W. G.: Bedrock Geology of New York City: More than 600 m.y. of geologic history" Field
861 Guide for Long Island Geologists Field Trip, October 27, 2001, in: *Field Guide for Long Island Geologists*
862 *Field Trip*, 2001.

863 Broecker, W. S. and Donk, J., van: Insolation changes, ice volumes, and the O18 record in deep-sea cores, *Rev*
864 *Geophys*, 8, 169–198, <https://doi.org/10.1029/rg008i001p00169>, 1970.

865 Bromley, G. R. M., Hall, B. L., Thompson, W. B., and Lowell, T. V.: Age of the Berlin moraine complex, New
866 Hampshire, USA, and implications for ice sheet dynamics and climate during Termination 1, *Quaternary*
867 *Res*, 94, 80–93, <https://doi.org/10.1017/qua.2019.66>, 2020.

868 Buizert, C., Gkinis, V., Severinghaus, J. P., He, F., Lecavalier, B. S., Kindler, P., Leuenberger, M., Carlson, A. E.,
869 Vinther, B., Masson-Delmotte, V., White, J. W. C., Liu, Z., Otto-Bliesner, B., and Brook, E. J.: Greenland
870 temperature response to climate forcing during the last deglaciation, *Science*, 345, 1177–1180,
871 <https://doi.org/10.1126/science.1254961>, 2014.

872 Cadwell, D.H.: Surficial Geologic Map of New York: Lower Hudson Sheet. New York State Museum Map and Chart
873 Series. The University of the State of New York, Albany, NY, 1989.

874 Clark, P. U., Dyke, A. S., Shakun, J. D., Carlson, A. E., Clark, J., Wohlfarth, B., Mitrovica, J. X., Hostetler, S. W.,

Deleted: <https://version2.ice-d.org/laurentide/>

Deleted: 26

Deleted: anuary

Deleted: ., 1998.

Deleted: .

Deleted: NY, 1989

881 and McCabe, A. M.: The Last Glacial Maximum, *Science*, 325, 710–714,
882 <https://doi.org/10.1126/science.1172873>, 2009.

883 Clark, P. U., Licciardi, J. M., MacAyeal, D. R., and Jenson, J. W.: Numerical reconstruction of a soft-bedded
884 Laurentide Ice Sheet during the last glacial maximum, *Geology*, 24, 679–682, 1996.

885 Clark, P. U., Marshall, S. J., Clarke, G. K. C., Hostetler, S. W., Licciardi, J. M., and Teller, J. T.: Freshwater Forcing
886 of Abrupt Climate Change During the Last Glaciation, *Science*, 293, 283–287,
887 <https://doi.org/10.1126/science.1062517>, 2001.

888 Collins, G.: The Very Cold Case of the Glacier. *The New York Times*, 2005.

889 Corbett, L. B., Bierman, P. R., Stone, B. D., Caffee, M. W., and Larsen, P. L.: Cosmogenic nuclide age estimate for
890 Laurentide Ice Sheet recession from the terminal moraine, New Jersey, USA, and constraints on latest
891 Pleistocene ice sheet history, *Quaternary Res.*, 87, 482–498, <https://doi.org/10.1017/qua.2017.11>, 2017.

892 Crump, S. E., Anderson, L. S., Miller, G. H., and Anderson, R. S.: Interpreting exposure ages from ice-cored moraines:
893 a Neoglacial case study on Baffin Island, Arctic Canada, *J. Quaternary Sci.*, 32, 1049–1062,
894 <https://doi.org/10.1002/jqs.2979>, 2017.

895 Cuffey, K. M., Clow, G. D., Steig, E. J., Buizert, C., Fudge, T. J., Koutnik, M., Waddington, E. D., Alley, R. B., and
896 Severinghaus, J. P.: Deglacial temperature history of West Antarctica, *Proc National Acad Sci*, 113, 14249–
897 14254, <https://doi.org/10.1073/pnas.1609132113>, 2016.

898 Curry, B. and Petras, J.: Chronological framework for the deglaciation of the Lake Michigan lobe of the Laurentide
899 Ice Sheet from ice-walled lake deposits, *J. Quaternary Sci.*, 26, 402–410, <https://doi.org/10.1002/jqs.1466>,
900 2011.

901 Dalton, A. S., Margold, M., Stokes, C. R., Tarasov, L., Dyke, A. S., Adams, R. S., Allard, S., Arends, H. E., Atkinson,
902 N., Attig, J. W., Barnett, P. J., Barnett, R. L., Batterson, M., Bernatchez, P., Borns, H. W., Breckenridge, A.,
903 Briner, J. P., Brouard, E., Campbell, J. E., Carlson, A. E., Clague, J. J., Curry, B. B., Daigneault, R.-A., Dubé-
904 Loubert, H., Easterbrook, D. J., Franzi, D. A., Friedrich, H. G., Funder, S., Gauthier, M. S., Gowan, A. S.,
905 Harris, K. L., Héту, B., Hooyer, T. S., Jennings, C. E., Johnson, M. D., Kehew, A. E., Kelley, S. E., Kerr, D.,
906 King, E. L., Kjeldsen, K. K., Knaeble, A. R., Lajeunesse, P., Lakeman, T. R., Lamothe, M., Larson, P.,
907 Lavoie, M., Loope, H. M., Lowell, T. V., Lusardi, B. A., Manz, L., McMartin, I., Nixon, F. C., Occhietti, S.,
908 Parkhill, M. A., Piper, D. J. W., Pronk, A. G., Richard, P. J. H., Ridge, J. C., Ross, M., Roy, M., Seaman, A.,
909 Shaw, J., Stea, R. R., Teller, J. T., Thompson, W. B., Thorleifson, L. H., Utting, D. J., Veillette, J. J., Ward,
910 B. C., Weddle, T. K., and Wright, H. E.: An updated radiocarbon-based ice margin chronology for the last
911 deglaciation of the North American Ice Sheet Complex, *Quaternary Sci Rev*, 234, 106223,
912 <https://doi.org/10.1016/j.quascirev.2020.106223>, 2020.

913 Davis, M. B., Spear, R. W., and Shane, L. C. K.: Holocene climate of New England, *Quat. Res.*, 14, 240–250,
914 [https://doi.org/10.1016/0033-5894\(80\)90051-4](https://doi.org/10.1016/0033-5894(80)90051-4), 1980.

915 Davis, P. T., Bierman, P. R., Corbett, L. B., and Finkel, R. C.: Cosmogenic exposure age evidence for rapid Laurentide
916 deglaciation of the Katahdin area, west-central Maine, USA, 16 to 15 ka, *Quaternary Sci Rev*, 116, 95–105,
917 <https://doi.org/10.1016/j.quascirev.2015.03.021>, 2015.

918 Deevey: Radiocarbon-dated pollen sequences in eastern North America, *Veroffentlichungen des Geobotanischen*
919 *Institutes Rubel in Zurich*, 30, 1958.

920 Denton, G. H. and Hughes, T. J.: *The Last Great Ice Sheets*, Wiley-Interscience, New York, 464 pp., 1981.

921 Denton, G. H., Anderson, R. F., Toggweiler, J. R., Edwards, R. L., Schaefer, J. M., and Putnam, A. E.: The Last
922 Glacial Termination, *Science*, 328, 1652–1656, <https://doi.org/10.1126/science.1184119>, 2010.

923 Dorion, C. C., Balco, G. A., Kaplan, M. R., Kreutz, K. J., Wright, ames D., and Jr., H. W. B.: Stratigraphy,
924 paleoceanography, chronology, and environment during deglaciation of eastern Maine, in: *Special papers*
925 *(Geological Society of America)*, vol. 351, edited by: Weddle, T. K. and Retelle, M. J., 215,
926 <https://doi.org/10.1130/0-8137-2351-5.215>, 2001.

927 Drebber, J. S., Halsted, C. T., Corbett, L. B., Bierman, P. R., and Caffee, M. W.: In Situ Cosmogenic ¹⁰Be Dating of
928 Laurentide Ice Sheet Retreat from Central New England, USA, *Geosciences*, 13, 213,

929 <https://doi.org/10.3390/geosciences13070213>, 2023.

930 Dyke, A. S.: An outline of North American deglaciation with emphasis on central and northern Canada, *Dev Quat Sci*,
931 2, 373–424, [https://doi.org/10.1016/s1571-0866\(04\)80209-4](https://doi.org/10.1016/s1571-0866(04)80209-4), 2004.

932 Frankel, L., and Thomas, H. F.: Evidence of freshwater lake deposits in Block Island Sound: *The Journal of Geology*,
933 v. 74, no. 2, p. 240–242, 1966.

934 Fuller, M. L.: *The Geology of Long Island New York*, US Geological Survey, 1914.

935 Glover, K. C., Lowell, T. V., Wiles, G. C., Pair, D., Applegate, P., and Hajdas, I.: Deglaciation, basin formation and
936 post-glacial climate change from a regional network of sediment core sites in Ohio and eastern Indiana, *Quat.*
937 *Res.*, 76, 401–410, <https://doi.org/10.1016/j.yqres.2011.06.004>, 2011.

938 Gregoire, L. J., Valdes, P. J., and Payne, A. J.: The relative contribution of orbital forcing and greenhouse gases to the
939 North American deglaciation, *Geophys Res Lett*, 42, 9970–9979, <https://doi.org/10.1002/2015gl066005>,
940 2015.

941 [Hall, B. L., Borns, H. W., Bromley, G. R. M., and Lowell, T. V.: Age of the Pineo Ridge System: Implications for](#)
942 [behavior of the Laurentide Ice Sheet in eastern Maine, U.S.A., during the last deglaciation, *Quaternary Sci*](#)
943 [Rev. 169, 344–356, <https://doi.org/10.1016/j.quascirev.2017.06.011>, 2017.](#)

944 Halsted, C. T., Bierman, P. R., Shakun, J. D., Davis, P. T., Corbett, L. B., Drebbler, J. S., and Ridge, J. C.: A critical
945 re-analysis of constraints on the timing and rate of Laurentide Ice Sheet recession in the northeastern United
946 States, *J. Quat. Sci.*, <https://doi.org/10.1002/jqs.3563>, 2023.

947 Halsted, C. T., Bierman, P. R., Shakun, J. D., Davis, P. T., Corbett, L. B., Caffee, M. W., Hodgdon, T. S., and Licciardi,
948 J. M.: Rapid southeastern Laurentide Ice Sheet thinning during the last deglaciation revealed by elevation
949 profiles of in situ cosmogenic ¹⁰Be, *Gsa Bulletin*, <https://doi.org/10.1130/b36463.1>, 2022.

950 Harbor, J., Stroeven, A. P., Fabel, D., Clarhäll, A., Kleman, J., Li, Y., Elmore, D., and Fink, D.: Cosmogenic nuclide
951 evidence for minimal erosion across two subglacial sliding boundaries of the late glacial Fennoscandian ice
952 sheet, *Geomorphology*, 75, 90–99, <https://doi.org/10.1016/j.geomorph.2004.09.036>, 2006.

953 Hays, J. D., Imbrie, J., and Shackleton, N. J.: Variations in the Earth's Orbit: Pacemaker of the Ice Ages, *Science*,
954 194, 1121–1132, <https://doi.org/10.1126/science.194.4270.1121>, 1976.

955 Heath, S. L., Loope, H. M., Curry, B. B., and Lowell, T. V.: Pattern of southern Laurentide Ice Sheet margin position
956 changes during Heinrich Stadials 2 and 1, *Quaternary Sci Rev*, 201, 362–379,
957 <https://doi.org/10.1016/j.quascirev.2018.10.019>, 2018.

958 Hooke, R. L., and H. B. Clausen: Wisconsin and holocene $\delta^{18}O$ variations, Barnes Ice Cap, Canada, *Geol. Soc. Am.*
959 *Bull.*, 93(8), 784–789, 1982.

960 Hooke, R. L.: Pleistocene ice and the base of the Barnes Ice Cap, Canada, *J. Glaciol.*, 17(75), 49–60, 1976.

961 Imbrie, J., Berger, A., Boyle, E. A., Clemens, S. C., Duffy, A., Howard, W. R., Kukla, G., Kutzbach, J., Martinson,
962 D. G., McIntyre, A., Mix, A. C., Molino, B., Morley, J. J., Peterson, L. C., Pisias, N. G., Prell, W. L., Raymo,
963 M. E., Shackleton, N. J., and Toggweiler, J. R.: On the structure and origin of major glaciation cycles 2. The
964 100,000-year cycle, *Paleoceanography*, 8, 699–735, <https://doi.org/10.1029/93pa02751>, 1993.

965 Jaret, S. J., Tailby, N. D., Hammond, K. G., Rasbury, E. T., Wootton, K., Ebel, D. S., DiPadova, E., Smith, R., Yuan,
966 V., Jaffe, N., Smith, L. M., and Spaeth, L.: Geology of Central Park, Manhattan, New York City, USA: New
967 geochemical insights, *The Geological Society of America Field Guide* 61, 1–14,
968 [https://doi.org/10.1130/2020.0061\(02\)](https://doi.org/10.1130/2020.0061(02)), 2021.

969 Kaplan, M. R., Strelin, J. A., Schaefer, J. M., Denton, G. H., Finkel, R. C., Schwartz, R., Putnam, A. E., Vandergoes,
970 M. J., Goehring, B. M., and Travis, S. G.: In-situ cosmogenic ¹⁰Be production rate at Lago Argentino,
971 Patagonia: Implications for late-glacial climate chronology, *Earth Planet Sc Lett*, 309, 21–32,
972 <https://doi.org/10.1016/j.epsl.2011.06.018>, 2011.

973 [Kaplan, M. R.: Retreat of a tidewater margin of the Laurentide ice sheet in eastern coastal Maine between ca. 14 000](#)
974 [and 13 000 ¹⁴C yr B.P., *GSA Bull.*, 111, 620–632, \[https://doi.org/10.1130/0016-\]\(https://doi.org/10.1130/0016-7606\(1999\)111<0620:roatmo>2.3.co;2\)](#)
975 [7606\(1999\)111<0620:roatmo>2.3.co;2, 1999.](#)

976 Kaye, C. A.: Early Postglacial Beavers in Southeastern New England, *Science*, 138, 906–907,

977 <https://doi.org/10.1126/science.138.3543.906>, 1962.

978 Kaye, C. A.: Geology of the Kingston Quadrangle, Rhode Island, Geological Survey Bulletin 1071-1, 15, 193–194,
979 1960.

980 Kaye, C. A.: Illinoian and early Wisconsinan moraines of Martha’s Vineyard, Massachusetts, US Geological Survey
981 Professional Paper 501-C., C140–C143, 1964a.

982 Kaye, C. A.: Outline of Pleistocene geology of Martha’s Vineyard, Massachusetts, US Geological Survey Professional
983 Paper 501-C, C134–C139, 1964b.

984 Kaye, C. A.: Preliminary surficial map of Martha’s Vineyard, Nomans Land, and parts of Naushon and Pasque Islands,
985 Massachusetts, US Geological Survey Open-File Report 72-205, 1972.

986 Kelly, M. A.: The Late Würmian Age in the Western Swiss Alps: Last Glacial Maximum (LGM) Ice-surface
987 Reconstruction and 10Be Dating of Late-glacial Features, 2003.

988 Kindler, P., Guillevic, M., Baumgartner, M., Schwander, J., Landais, A., and Leuenberger, M.: Temperature
989 reconstruction from 10 to 120 kyr b2k from the NGRIP ice core, *Clim Past*, 10, 887–902,
990 <https://doi.org/10.5194/cp-10-887-2014>, 2014.

991 Koteff, C. and Jr., F. P.: Systematic Ice Retreat in New England, in: Geological Survey Professional Paper 1179,
992 United States Government Printing Office, Washington, 1981.

993 Lal, D.: Cosmic ray labeling of erosion surfaces: in situ nuclide production rates and erosion models, *Earth Planet Sc
994 Lett*, 104, 424–439, [https://doi.org/10.1016/0012-821x\(91\)90220-c](https://doi.org/10.1016/0012-821x(91)90220-c), 1991.

995 Lambeck, K., Rouby, H., Purcell, A., Sun, Y., and Sambridge, M.: Sea level and global ice volumes from the Last
996 Glacial Maximum to the Holocene, *Proc National Acad Sci*, 111, 15296–15303,
997 <https://doi.org/10.1073/pnas.1411762111>, 2014.

998 Laskar, J., Robutel, P., Joutel, F., Gastineau, M., Correia, A. C. M., and Levrard, B.: A long-term numerical solution
999 for the insolation quantities of the Earth, *Astron Astrophys*, 428, 261–285, <https://doi.org/10.1051/0004-6361:20041335>, 2004.

1000

1001 Lifton, N., Sato, T., and Dunai, T. J.: Scaling in situ cosmogenic nuclide production rates using analytical
1002 approximations to atmospheric cosmic-ray fluxes, *Earth Planet Sc Lett*, 386, 149–160,
1003 <https://doi.org/10.1016/j.epsl.2013.10.052>, 2014.

1004 Löfverström, M., Caballero, R., Nilsson, J., and Kleman, J.: Evolution of the large-scale atmospheric circulation in
1005 response to changing ice sheets over the last glacial cycle, *Clim Past*, 10, 1453–1471,
1006 <https://doi.org/10.5194/cp-10-1453-2014>, 2014.

1007 Marcott, S. A., Bauska, T. K., Buizert, C., Steig, E. J., Rosen, J. L., Cuffey, K. M., Fudge, T. J., Severinghaus, J. P.,
1008 Ahn, J., Kalk, M. L., McConnell, J. R., Sowers, T., Taylor, K. C., White, J. W. C., and Brook, E. J.:
1009 Centennial-scale changes in the global carbon cycle during the last deglaciation, *Nature*, 514, 616–619,
1010 <https://doi.org/10.1038/nature13799>, 2014.

1011 McManus, J. F., Francois, R., Gherardi, J.-M., Keigwin, L. D., and Brown-Leger, S.: Collapse and rapid resumption
1012 of Atlantic meridional circulation linked to deglacial climate changes, *Nature*, 428, 834–837,
1013 <https://doi.org/10.1038/nature02494>, 2004.

1014 McMaster, R. L.: Sediments of Narragansett Bay system and Rhode Island Sound, Rhode Island, *J Sediment Res*, 30,
1015 249–274, <https://doi.org/10.1306/74d70a15-2b21-11d7-8648000102c1865d>, 1960.

1016 McWeeny, L. J.: Revised vegetation history for the post-glacial period (15,200–10,000 14 C years B.P.) in southern
1017 New England, in: Geological Society of America Abstracts with Programs 27, 1995.

1018 Milankovitch, M.: Kanon der Erdbestrahlung und Seine Anwendung auf das Eiszeitenproblem, Special Publication.
1019 Royal Serbian Academy, 33, 132, 1941.

1020 Mills, H. C. and Wells, P. D.: Ice-Shove Deformation and Glacial Stratigraphy of Port Washington, Long Island, New
1021 York, *Gsa Bulletin*, 85, 357–364, [https://doi.org/10.1130/0016-7606\(1974\)85<357:idadgso>2.0.co;2](https://doi.org/10.1130/0016-7606(1974)85<357:idadgso>2.0.co;2), 1974.

1022 NASA Shuttle Radar Topography Mission (SRTM). Shuttle Radar Topography Mission (SRTM) Global.
1023 Distributed by OpenTopography. <https://doi.org/10.5069/G9445JDF>. last access: 26 January 2024.

- 1024 Needell, S. W., O'Hara, C. J., and Knebel, H. J.: Quaternary geology of the Rhode Island inner shelf: *Marine Geology*,
 1025 v. 53, p. 41-53, 1983.
- 1026 Nishiizumi, K., Imamura, M., Caffee, M. W., Southon, J. R., Finkel, R. C., and McAninch, J.: Absolute calibration of
 1027 ¹⁰Be AMS standards, *Nucl Instruments Methods Phys Res Sect B Beam Interactions Mater Atoms*, 258,
 1028 403–413, <https://doi.org/10.1016/j.nimb.2007.01.297>, 2007.
- 1029 Nishiizumi, K.: ¹⁰Be, ²⁶Al, ³⁶Cl, and ⁴¹Ca AMS standards, in: 9th Conference on Accelerator Mass Spectrometry.
 1030 p. 130, 2002.
- 1031 Oakley, B. A. and Boothroyd, J. C.: Constrained age of Glacial Lake Narragansett and the deglacial chronology of the
 1032 Laurentide Ice Sheet in southeastern New England, *J Paleolimnol*, 50, 305–317,
 1033 <https://doi.org/10.1007/s10933-013-9725-7>, 2013.
- 1034 Oakley, B. A.: Late Quaternary Depositional Environments, Timing and Recent Deposition: Narragansett Bay, Rhode
 1035 Island and Massachusetts, Doctoral thesis, University of Rhode Island, 2012.
- 1036 Oldale, R. N. and O'Hara, C. J.: Glaciotectonic origin of the Massachusetts coastal end moraines and a fluctuating
 1037 late Wisconsinan ice margin, *GSA Bulletin*, 95, 61–74, [https://doi.org/10.1130/0016-7606\(1984\)95<61:gootmc>2.0.co;2](https://doi.org/10.1130/0016-7606(1984)95<61:gootmc>2.0.co;2), 1984.
- 1039 Oldale, R. N.: Pleistocene stratigraphy of Nantucket, Martha's Vineyard, the Elizabeth Islands, and Cape Cod,
 1040 Massachusetts, in: Late Wisconsinan Glaciation of New England: Proceedings of the Symposium, edited by:
 1041 Larson, G. J. and Stone, B. D., Kendall/Hunt, Dubuque, IA, 1–34, 1982.
- 1042 Peteet, D. M., Beh, M., Orr, C., Kurdyla, D., Nichols, J., and Guilderson, T.: Delayed deglaciation or extreme Arctic
 1043 conditions 21-16 cal. kyr at southeastern Laurentide Ice Sheet margin?, *Geophys Res Lett*, 39, n/a-n/a,
 1044 <https://doi.org/10.1029/2012gl051884>, 2012.
- 1045 [Prince, K. K., Briner, J. P., Walcott, C. K., Chase, B. M., Kozłowski, A. L., Rittenour, T. M., and Yang, E. P.: New](https://doi.org/10.5194/egusphere-2023-2655)
 1046 [age constraints reveal moraine stabilization thousands of years after deposition during the last deglaciation](https://doi.org/10.5194/egusphere-2023-2655)
 1047 [of western New York, USA, EGU sphere \[preprint\], https://doi.org/10.5194/egusphere-2023-2655, 2024.](https://doi.org/10.5194/egusphere-2023-2655)
- 1048 Putnam, A. E., Bromley, G. R. M., Rademaker, K., and Schaefer, J. M.: In situ ¹⁰Be production-rate calibration from
 1049 a ¹⁴C-dated late-glacial moraine belt in Rannoch Moor, central Scottish Highlands, *Quat Geochronol*, 50,
 1050 109–125, <https://doi.org/10.1016/j.quageo.2018.11.006>, 2019.
- 1051 Raymo, M. E.: The timing of major climate terminations, *Paleoceanography*, 12, 577–585,
 1052 <https://doi.org/10.1029/97pa01169>, 1997.
- 1053 Refsnider, K.A., Miller, G.H., Fogel, M.L., Fréchet, B., Bowden, R., Andrews, J.T., Farmer, G.L.: Subglacially
 1054 precipitated carbonates record geochemical interactions and pollen preservation at the base of the Laurentide
 1055 Ice Sheet on central Baffin Island, eastern Canadian Arctic. *Quaternary Res* 81, 94–105.
 1056 <https://doi.org/10.1016/j.yqres.2013.10.014>, 2014.
- 1057 Reimer, G. E.: The Sedimentology and Stratigraphy of the Southern Basin of Glacial Lake Passaic, New Jersey,
 1058 Master's thesis, Rutgers University, New Brunswick, New Jersey, 1984.
- 1059 Reimer, P. J., Austin, W. E. N., Bard, E., Bayliss, A., Blackwell, P. G., Ramsey, C. B., Butzin, M., Cheng, H., Edwards,
 1060 R. L., Friedrich, M., Grootes, P. M., Guilderson, T. P., Hajdas, I., Heaton, T. J., Hogg, A. G., Hughen, K. A.,
 1061 Kromer, B., Manning, S. W., Muscheler, R., Palmer, J. G., Pearson, C., Plicht, J. van der, Reimer, R. W.,
 1062 Richards, D. A., Scott, E. M., Southon, J. R., Turney, C. S. M., Wacker, L., Adolphi, F., Büntgen, U., Capano,
 1063 M., Fahrni, S. M., Fogtmann-Schulz, A., Friedrich, R., Köhler, P., Kudsk, S., Miyake, F., Olsen, J., Reinig,
 1064 F., Sakamoto, M., Sookdeo, A., and Talamo, S.: The IntCal20 Northern Hemisphere Radiocarbon Age
 1065 Calibration Curve (0–55 cal kBP), *Radiocarbon*, 62, 725–757, <https://doi.org/10.1017/rdc.2020.41>, 2020.
- 1066 Ridge, J. C., Balco, G., Bayless, R. L., Beck, C. C., Carter, L. B., Dean, J. L., Voytek, E. B., and Wei, J. H.: The new
 1067 North American Varve Chronology: A precise record of southeastern Laurentide Ice Sheet deglaciation and
 1068 climate, 18.2-12.5 kyr BP, and correlations with Greenland ice core records, *Am J Sci*, 312, 685–722,
 1069 <https://doi.org/10.2475/07.2012.01>, 2012.
- 1070 Ridge, J. C.: The Quaternary glaciation of western New England with correlations to surrounding areas, *Dev Quat*
 1071 *Sci*, 2, 169–199, [https://doi.org/10.1016/s1571-0866\(04\)80196-9](https://doi.org/10.1016/s1571-0866(04)80196-9), 2004.

Formatted: Font: (Default) Times New Roman, 10 pt, Font color: Auto, Pattern: Clear

1072 Rittenour, T.M., Stone, B.D., and Mahan, S.: Application of OSL dating to glacial deposits in southern Massachusetts:
1073 Refining the chronology and addressing questions related to solar resetting in glacial environments,
1074 Geological Society of America Abstracts with Programs, 44 (2), p. 86, 2012.

1075 Schaefer, J. M., Denton, G. H., Kaplan, M., Putnam, A., Finkel, R. C., Barrell, D. J. A., Andersen, B. G., Schwartz,
1076 R., Mackintosh, A., Chinn, T., and Schlüchter, C.: High-Frequency Holocene Glacier Fluctuations in New
1077 Zealand Differ from the Northern Signature, *Science*, 324, 622–625,
1078 <https://doi.org/10.1126/science.1169312>, 2009.

1079 Schafer, J. P. and Hartshorn, J. H.: The Quaternary of New England, in: *The Quaternary of the United States*, edited
1080 by: Jr., H. E. W. and Frey, D. G., Princeton University Press, Princeton, NJ, 113–127, 1965.

1081 Schafer, J. P.: Surficial Geologic Map of the Watch Hill quadrangle, Rhode Island-Connecticut, scale 1:24,000, 1965.

1082 Schuldenrein, J. and Aiuvalasit, M.: Urban geoarchaeology and sustainability: A case study from Manhattan Island,
1083 New York City, USA, in: *Geoarchaeology, Climate Change, and Sustainability: Geological Society of
1084 America Special Paper 476*, edited by: Brown, A. G., Basell, L. S., and Butzer, K. W.,
1085 [https://doi.org/10.1130/2011.2476\(12\)](https://doi.org/10.1130/2011.2476(12)), 2011.

1086 Shakun, J. D., Clark, P. U., He, F., Lifton, N. A., Liu, Z., and Otto-Bliesner, B. L.: Regional and global forcing of
1087 glacier retreat during the last deglaciation, *Nat Commun*, 6, 8059, <https://doi.org/10.1038/ncomms9059>,
1088 2015.

1089 Sinclair, S. N., Licciardi, J. M., Campbell, S. W., and Madore, B. M.: Character and origin of De Geer moraines in
1090 the Seacoast region of New Hampshire, USA: *Journal of Quaternary Science*, v. 33, no. 2, p. 225-237, 2018.

1091 Sirkin, L. and Stuckenrath, R.: The Portwashingtonian warm interval in the northern Atlantic coastal plain, *GSA
1092 Bulletin*, 91, 332–336, [https://doi.org/10.1130/0016-7606\(1980\)91<332:tpwiit>2.0.co;2](https://doi.org/10.1130/0016-7606(1980)91<332:tpwiit>2.0.co;2), 1980.

1093 Sirkin, L., 1986. Pleistocene stratigraphy of Long Island, New York, in: Cadwell, D.H. (Eds.), *The Wisconsinan Stage
1094 of the First Geological District, Eastern New York*. New York State Museum, Albany, NY.

1095 Sirkin, L.: Block Island, Rhode Island: Evidence of fluctuation of the late Pleistocene ice margin, *GSA Bulletin*, 87,
1096 574–580, [https://doi.org/10.1130/0016-7606\(1976\)87<574:birieo>2.0.co;2](https://doi.org/10.1130/0016-7606(1976)87<574:birieo>2.0.co;2), 1976.

1097 Sirkin: Late Wisconsinan glaciation of Long Island, New York, to Block Island, Rhode Island, 35–59, 1982.

1098 Soren, J.: Geologic and geohydrologic reconnaissance of Staten Island, New York, U.S Geological Survey, Water-
1099 Resources Investigations Report 87-4048, <https://doi.org/10.3133/wri874048>, 1988.

1100 Stanford, S. D. and Harper, D.: Glacial lakes of the lower Passaic, 13, 271–286, 1991.

1101 Stanford, S. D., Stone, B. D., Ridge, J. C., Witte, R. W., Pardi, R. R., and Reimer, G. E.: Chronology of Laurentide
1102 glaciation in New Jersey and the New York City area, United States, *Quaternary Res*, 99, 142–167,
1103 <https://doi.org/10.1017/qua.2020.71>, 2021.

1104 Stanford, S. D.: Late Wisconsinan glacial geology of the New Jersey Highlands, *Northeastern Geology*, 210–223,
1105 1993.

1106 Stanford, S. D.: Onshore record of Hudson River drainage to the continental shelf from the late Miocene through the
1107 late Wisconsinan deglaciation, U.S.A.: synthesis and revision, *Boreas*, 1–17, 2010.

1108 Stokes, C. R., Tarasov, L., and Dyke, A. S.: Dynamics of the North American Ice Sheet Complex during its inception
1109 and build-up to the Last Glacial Maximum, *Quaternary Sci Rev*, 50, 86–104,
1110 <https://doi.org/10.1016/j.quascirev.2012.07.009>, 2012.

1111 Stokes, C. R.: Deglaciation of the Laurentide Ice Sheet from the Last Glacial Maximum, *Cuadernos De Investigación
1112 Geográfica*, 43, 377–428, <https://doi.org/10.18172/cig.3237>, 2017.

1113 Stone, B. D. and Borns, H. W. Jr.: Pleistocene glacial and interglacial stratigraphy of New England, Long Island, and
1114 adjacent Georges Bank and Gulf of Maine, *Quaternary Sci Rev*, 5, 39–52, [https://doi.org/10.1016/0277-3791\(86\)90172-1](https://doi.org/10.1016/0277-3791(86)90172-1), 1986.

1116 Stone, B. D., Stanford, S. D., and Witte, R. W.: Surficial Geologic Map of Northern New Jersey, Miscellaneous
1117 Investigations Series Map I-2540-C, U.S. Geological Survey, Reston, VA, 2002.

1118 Stone, B. D., Stanford, S. D., and Witte, R. W.: Surficial Geologic Map of the Northern Sheet, New Jersey, US
1119 Geological Survey, U.S. Geological Survey Open File Map OF 95-543B, 1995.

1120 Stone, B.D., and Stone, J.R.: Geologic Origins of Cape Cod, Massachusetts; Guidebook for the Northeast Friends of
1121 the Pleistocene, 82 nd Annual Fieldtrip, May 31-June 2, 2019: Massachusetts Geological Survey Open-file
1122 Report 19-01, 63 p, <https://www2.newpaltz.edu/fop/pdf/FOP2019Guide.pdf>, 2019.

1123 Stone, J. R., Stone, B. D., DiGiacomo-Cohen, M. L., and Mabee, S. B.: Surficial Materials of Massachusetts— A
1124 1:24,000-Scale Geologic Map Database, USGS Scientific Investigations Map 3402,
1125 <https://doi.org/10.3133/sim3402>, 2018.

1126 Stone, J. O., Balco, G. A., Sugden, D. E., Caffee, M. W., III, L. C. S., Cowdery, S. G., and Siddoway, C.: Holocene
1127 Deglaciation of Marie Byrd Land, West Antarctica, *Science*, 299, 99–102,
1128 <https://doi.org/10.1126/science.1077998>, 2003.

1129 Stone, J. O.: Air pressure and cosmogenic isotope production, *J Geophys Res Solid Earth*, 105, 23753–23759,
1130 <https://doi.org/10.1029/2000jb900181>, 2000.

1131 Stone, J. R., Schafer, J. P., London, E. H., DiGiacomo-Cohen, M. L., Lewis, R. S., and Thompson, W. B.: Quaternary
1132 Geologic Map of Connecticut and Long Island Sound Basin, U.S. Geological Survey, 2005.
1133 <https://doi.org/10.3133/sim2784>

1134 Stone, J. R., Shafer, J. P., London, E. H., DiGiacomo-Cohen, M., Lewis, R. S., and Thompson, W. B.: Quaternary
1135 Geologic Map of Connecticut and Long Island Sound Basin: : U.S. Geological Survey Geologic
1136 Investigations Series Map I-2784, scale 1:125,000, 2 sheets and pamphlet. p. 1-72, 2005.

1137 Stone, J. R.: Surficial Materials Map of the Chipuxet River and Chickasheen Brook Basins, Rhode Island, U.S.
1138 Geological Survey, 2014.

1139 Taterka, B. D.: Bedrock geology of Central Park, New York City, M.S. Thesis University of Massachusetts Depart-
1140 ment of Geology and Geography, Contribution 61, 1987.

1141 Todd, B. J., Valentine, P. C., Longva, O., and Shaw, J.: Glacial landforms on German Bank, Scotian Shelf: evidence
1142 for Late Wisconsinan ice-sheet dynamics and implications for the formation of De Geer moraines: *Boreas*,
1143 v. 36, no. 2, p. 148-169, 2007.

1144 Tucholke and Hollister, B. E.: Late Wisconsin glaciation of the southwestern Gulf of Maine: new evidence from the
1145 marine environment, *GSA Bulletin* 84, 279–3296, 1973.

1146 Tzedakis, P. C., Drysdale, R. N., Margari, V., Skinner, L. C., Menviel, L., Rhodes, R. H., Taschetto, A. S., Hodell, D.
1147 A., Crowhurst, S. J., Hellstrom, J. C., Fallick, A. E., Grimalt, J. O., McManus, J. F., Martrat, B., Mokeddem,
1148 Z., Parrenin, F., Regattieri, E., Roe, K., and Zanchetta, G.: Enhanced climate instability in the North Atlantic
1149 and southern Europe during the Last Interglacial, *Nat Commun*, 9, 4235, [https://doi.org/10.1038/s41467-018-](https://doi.org/10.1038/s41467-018-06683-3)
1150 [06683-3](https://doi.org/10.1038/s41467-018-06683-3), 2018.

1151 Ullman, D. J., Carlson, A. E., LeGrande, A. N., Anslow, F. S., Moore, A. K., Caffee, M., Syverson, K. M., and
1152 Licciardi, J. M.: Southern Laurentide ice-sheet retreat synchronous with rising boreal summer insolation,
1153 *Geology*, 43, 23–26, <https://doi.org/10.1130/g36179.1>, 2015.

1154 Ullman, D. J., LeGrande, A. N., Carlson, A. E., Anslow, F. S., and Licciardi, J. M.: Assessing the impact of Laurentide
1155 Ice Sheet topography on glacial climate, *Clim Past*, 10, 487–507, <https://doi.org/10.5194/cp-10-487-2014>,
1156 2014.

1157 Upham, W.: Terminal moraines of the North American ice sheet, *American Journal of Science*, s3-18, 197,
1158 <https://doi.org/10.2475/ajs.s3-18.105.197>, 1879.

1159 Woodworth, J. B. and Wigglesworth, E.: Geography and geology of the region including Cape Cod, the Elizabeth
1160 islands, Nantucket, Marthas Vineyard, No Mans Land and Block Island, by J. B. Woodworth and Edward
1161 Wigglesworth, Printed for the Museum, Cambridge, Mass, 1934.

1162 Wroblewski, E. A., and Hooke, R. L.: Deglaciation of Penobscot Bay, Maine, USA: *Atlantic Geology*, v. 56, p. 147-
1163 161, 2020.

1164 Young, N. E., Briner, J. P., Maurer, J., and Schaefer, J. M.: 10Be measurements in bedrock constrain erosion beneath
1165 the Greenland Ice Sheet margin, *Geophys Res Lett*, 43, 11,708-11,719,
1166 <https://doi.org/10.1002/2016gl070258>, 2016.

1167 Young, N. E., Schaefer, J. M., Briner, J. P., and Goehring, B. M.: A 10Be production-rate calibration for the Arctic, *J*

Deleted: <https://doi.org/10.3133/gq474>

Formatted: Font: Times New Roman, 10 pt, No underline,
Font color: Auto, Pattern: Clear

Formatted: Font: Times New Roman, 10 pt, No underline,
Font color: Auto, Pattern: Clear

1169 Quaternary Sci, 28, 515–526, <https://doi.org/10.1002/jqs.2642>, 2013.
1170
1171
1172
1173

